

Supporting Information

Yttrium-mediated ring-opening polymerization of functionalizable dihydrocarvide: tunable terpene-based polyesters using grafting from and block copolymerization strategies

*Lea-Sophie Hornberger, Julian Fischer, Alexandra Friedly, Ingo Hartenbach, Thomas Sottmann, Friederike Adams**

1. Experimental Section

Materials:

All chemicals were purchased from *Sigma-Aldrich*, *fisher scientific*, *TCI chemicals*, or other chemical suppliers and, unless otherwise stated, used as received: (+)-dihydrocarvone (mixture of isomers, 99.5 %, *Sigma-Aldrich*), Oxone (monopersulfate, *abcr*), sodium hydrogen carbonate (p.a., *CHEMSOLUTE*), sodium bisulfite (ACS reagent, *Sigma-Aldrich*), 2-propanol (anhydrous, 99.5 %, *Sigma-Aldrich*), 15-pentadecalactone (> 98 %, *TCI America*), β -butyrolactone (98 %, *Sigma-Aldrich*), 2-mercaptoethanol (> 98.0 %, *TCI*), 2,2-dimethoxy-2-phenylacetophenone (99 %, *Aldrich*), triethylamine (puriss, > 99.0 %, *CHEMSOLUTE*), 2-bromoisobutyryl bromide, > 98.0 %, *TCI*), ethyl acrylate (stabilized with MEHQ, > 99.0 %, *TCI*), ethyl 2-bromoisobutyrate (> 98 %, *TCI*), copper(II) bromide (99.999 %, *Sigma-Aldrich*), tris[2-(dimethylamino)ethyl]amine (> 98%, *TCI*), silica (60 M, 0.004-0.063 mm, *Macherey-Nagel*), aluminum oxide (90 neutral, activity 1, *Macherey-Nagel*), hydrochloric acid 37% (AnalaR NORMAPUR, Reag. Ph. Eur., *VWR*), acetone (techn. grade, *SCHARR*), methanol (techn. grade, *SCHARR*), diethyl ether (techn. grade, *SCHARR*), ethyl acetate (techn. grade, distilled before use, *SCHARR*), dichloromethane (techn. grade, *SCHARR*), benzene (ROTIPURAN, \geq 99.5 %, p.a., *Carl Roth*), N,N-dimethylformamide (extra dry over molecular sieve, AcroSeal, 99.8 %, *thermo scientific*), chloroform (puriss. p.a., reag. ISO, reag. Ph. Eur., 99.0 – 99.4 % (GC), *Sigma-Aldrich*), n-hexane (AnalaR NORMAPUR, Reag. Ph. Eur., ACS, 99.0 %, *VWR*), tetrahydrofuran (stabilized with BHT, ACS reagent, 99.6 %, *thermo scientific*). Toluene (EMSURE, ACS, ISO, Reag. Ph. Eur., *Merck*) was dried with a solvent purification system (*MBraun*) and stored over molecular sieves inside an argon-filled glovebox (*MBraun EcoLab*).

Copper wire (d = 0.25 mm, Puratronic, 99.9985 %, metals basis) and silver powder (spherical, APS 0.5-1 micron, 99.9%, metals basis) were purchased from *Thermo Fisher Scientific*. The copper wire was cleaned prior to use by treatment with concentrated hydrochloric acid, followed by two successive washes with demineralized water and two subsequent washes with acetone.

The synthesis of the yttrium-bdsa-precursor (Y(bdsa)₃(THF)₂, (bdsa = bis(dimethylsilyl)amide)¹, the 2-methoxyethylamino-bis(phenolate) ligand² and the amino-alkoxy-bis(phenolate) yttrium amido catalyst [(ONOO)^{tBu}Y(bdsa)(THF)]³ were performed according to literature. 2-(Pyridin-2-yl)disulfanyl ethanol was synthesized from 2,2'-dithiodipyridine according to literature synthesis.⁴ TPMA^{NMe2} was synthesized following a previously reported literature procedure.⁵

All polymerization reactions were performed under an argon atmosphere in a glovebox. Before use, racemic β -butyrolactone (BBL) was stirred over barium oxide (BaO). After the separation of the BBL from BaO via centrifugation, BBL was dried over calcium hydride and distilled. ω -Pentadecalactone (PDL) was dried under vacuum using a Schlenk line setup.

Analysis:

Nuclear magnetic resonance (NMR) spectra were acquired utilizing a *Bruker Avance III 400* or *Bruker Avance III HD 700* NMR spectrometer. Chemical shifts in parts per million (ppm) were referenced to the residual proton signal of the deuterated solvent employed for substance dissolution.

Size exclusion chromatography (SEC) was performed using chloroform on a SEC setup containing one PSS SDV 5 μm 8*50 mm guard column coupled with three PSS SDV 100,000 \AA 5 μm 8*50 mm columns, all heated at 40 $^{\circ}\text{C}$. The columns were connected with an Agilent 1200 Series G1362A refractive index (RI) detector. All samples had concentrations around 3 mg mL^{-1} . SEC measurements were performed at a flow rate of 1 mL min^{-1} . Relative molar masses were determined using polystyrene standards.

Differential scanning calorimetry (DSC) was measured with a PerkinElmer DSC 4000 with sample weights between 5 and 10 mg. The instrument was calibrated using indium (melting point: 159.63 $^{\circ}\text{C}$, enthalpy of fusion: 27.18 J g^{-1}). Measurements were conducted in an endo-up mode, employing a heating/cooling rate of 10 K min^{-1} over two cycles. The second heating cycle was always used for evaluation.

Gas chromatography-mass spectrometry (GC-MS) analysis was executed on a 5977D GC system by Agilent. Samples were dissolved in acetone with a concentration of 2 mg mL^{-1} .

Electrospray ionization coupled with mass spectrometry (ESI-MS) measurements were conducted in acetonitrile using either a Varian 500-MS spectrometer or a micrOTOF-Q Bruker Daltonics in positive ionization mode.

Positive ion matrix-assisted laser desorption ionization time-of-flight (MALDI-TOF) measurements were carried out using a Bruker Autoflex III with a smart beam in reflector mode. Samples were prepared from tetrahydrofuran solutions. The 2,5-dihydrobenzoic acid matrix (5 mg mL^{-1} in thf) was mixed with the sample (5 mg mL^{-1} in thf) and sodium trifluoromethanesulfonate (0.1 M in 90 % acetone, 10 % water) in a ratio of 2:1:2.

Powder X-ray diffraction (PXRD) was measured with Cu-K α radiation using a Rigaku SmartLab equipped with a Hypix3000 detector. All measurements were carried out in the reflection geometry. Baseline correction was performed manually.

Small-angle X-ray scattering (SAXS) measurements were performed with the Xeuss 3.0 UHR diffractometer from Xenocs, equipped with a GeniX 3D X-ray source (Cu K α ; $\lambda = 1.54 \text{\AA}$), double slit collimation, and an EIGER2 S IM 2D-detector from Dectris. The instrument was calibrated using lanthanum hexaboride (LaB $_6$) as a reference. The polymer samples were prepared with a thickness of 0.5 mm and mounted in a cell between two Kapton foil windows (12.5 μm thickness). The measurements were carried out at room temperature with sample-to-detector distances of 4500, 3500, 1500, 500, 100, and 50 mm and an exposure time of 4800 s for each distance. The 2D scattering patterns were radially averaged as a function of the momentum transfer $q = 4\pi \sin(\theta)/\lambda$ (scattering angle 2θ), resulting in q -ranges between 3×10^{-3} and 3\AA^{-1} . The recorded scattering intensities were normalized to an absolute scale using glassy carbon measurements. All data were reduced considering empty cell scattering as well as the direct beam transmission using the software X S ACT from Xenocs.

Synthesis of Dihydrocarvide:

Dihydrocarvide, obtained in the form of a colorless oil, was synthesized from dihydrocarvone. (+)-Dihydrocarvone, acquired as an isomeric mixture from Sigma-Aldrich (batch number SHBL6822) was utilized without further purification. The synthesis was performed according to literature.⁶ The product, which was the *trans* isomer (4R,7R)-4-isopropenyl-7-methyloxepan-2-one ((4R,7R)-dihydrocarvide, DHC), was analyzed using NMR spectroscopy, GC-MS, and elemental analysis.

¹H NMR (400 MHz, CDCl₃, 298 K): δ [ppm] = 4.69 (d, *J* = 8.1 Hz, 2H), 4.43 (dq, *J* = 8.9, 6.4 Hz, 1H), 2.88 – 2.43 (m, 2H), 2.24 (tdd, *J* = 10.6, 3.4, 1.7 Hz, 1H), 1.99 – 1.81 (m, 2H), 1.68 (s, 3H), 1.67 – 1.49 (m, 2H), 1.31 (d, *J* = 6.4 Hz, 3H).

Elemental Analysis of *trans*-Dihydrocarvide:

	Calculated [%]	Found [%]
C	71.39	71.37
H	9.63	9.57

Homopolymerization of Dihydrocarvide in Toluene with [(ONOO)^tBuY(bdsa)(THF)]:

Dihydrocarvide was weighed, stirred, and pre-heated to the reaction temperature (room temperature or 60 °C). A solution of 19.94 mg [(ONOO)^tBuY(bdsa)(THF)] (24.9 μmol, 1.0 eq., 19.94 mg) in 0.5 mL toluene was prepared and stirred at the polymerization temperature for five minutes. Subsequently, the catalyst solution was added to the dihydrocarvide in a single addition. The resulting mixture was stirred at the reaction temperature (room temperature or 60 °C) for 2 hours. A 0.05 mL aliquot was withdrawn for conversion determination by ¹H NMR spectroscopy integrating the –C–H– groups of DHC and PDHC. The polymerization reaction was quenched by the addition of 20 mL of cold methanol, followed by decantation of the supernatant. The remaining precipitate (colorless to yellowish) was dried in a vacuum oven (60 °C, 200 mbar) overnight. The resulting PDHC was analyzed by NMR spectroscopy and SEC in chloroform, which was employed for the determination of relative molar masses and polydispersities.

¹H NMR (400 MHz, CDCl₃, 298 K): δ [ppm] = 4.91 – 4.80 (m, 1H), 4.74 (d, *J* = 14.1 Hz, 2H), 2.64 – 2.43 (m, 1H), 2.30 (dd, *J* = 7.6, 1.3 Hz, 2H), 1.63 (s, 3H), 1.56 – 1.23 (m, 4H), 1.16 (d, *J* = 6.2 Hz, 3H).

Elemental Analysis of Poly(dihydrocarvide):

	Calculated [%]	Found [%]
C	71.39	71.25
H	9.59	9.69

Homopolymerization of Dihydrocarvide Carried out as a Neat Reaction:

9.94 mg [(ONOO)^tBuY(bdsa)(THF)] (24.9 μmol, 1.0 eq., 19.94 mg) was weighed and stirred at 60 °C. The dihydrocarvide was quantitatively measured in a syringe and introduced in a single addition to the catalyst. The reaction mixture was stirred at 60 °C for 2 hours. Before quenching the reaction with 20 mL of cold methanol, a sample was extracted using a spatula to determine the conversion by ¹H NMR spectroscopy. After removal of the supernatant, the residue was dried under vacuum (60 °C, 200 mbar) overnight. The obtained PDHC polymer was isolated in a quantitative yield and subsequently analyzed using NMR spectroscopy and SEC in chloroform.

Homopolymerization of Dihydrocarvide in Toluene with a Chain Transfer Agent or in situ Preparation of [(ONOO)^tBuY(iPrO)(THF)] Catalyst:

Polymerizations with a chain transfer agent were performed as the homopolymerization described above, but an extra step was added. The monomer was weighed and stirred at 60 °C and in an extra vial the [(ONOO)^tBuY(bdsa)(THF)] catalyst was weighed and dissolved in 0.5 mL toluene. The respective amount of

isopropanol was added to the catalyst solution and this mixture was stirred for a further 5 min at 60 °C. For the in situ preparation of the alkoxide catalyst only 1 eq. of isopropanol in comparison to the bdsa-complex was added. This mixture was added to the monomer in one shot to start the polymerization followed by the further steps as described above for the homopolymerization with [(ONOO)^{tBu}Y(bdsa)(THF)].

Kinetic Measurements for the Dihydrocarvide Polymerization with [(ONOO)^{tBu}Y(bdsa)(THF)] or [(ONOO)^{tBu}Y(iPrO)(THF)] Catalyst:

An aliquot method was employed for kinetic measurements of the dihydrocarvide polymerization. Dihydrocarvide (2.49 mmol, 50 eq., 418.57 mg) was weighed, dissolved in 3 mL toluene, and stirred at the reaction temperature (room temperature or 60 °C). The [(ONOO)^{tBu}Y(bdsa)(THF)] catalyst (49.8 μmol, 1.0 eq., 39.78 mg) was dissolved in 1 mL toluene and in case of polymerization with [(ONOO)^{tBu}Y(iPrO)(THF)], isopropanol (49.8 μmol, 1eq., 3.84 μmol) was added. The resulting mixture was stirred at 60 °C for 5 minutes and added in a single addition to the monomer solution. At regular time intervals, 100 μL aliquots were taken from the polymerization mixture and quenched by the addition of 0.5 mL wet CDCl₃. The conversion was determined through ¹H NMR spectroscopy, while the relative molar mass and polydispersity of each sample was analyzed using SEC in chloroform.

Block Copolymerization of ω-Pentadecalactone and Dihydrocarvide:

Block copolymers were synthesized via the sequential addition of monomers. The respective amount of ω-pentadecalactone was dissolved in 1.5 mL of toluene and stirred in a heating block at 60 °C. The catalyst solution of 19.94 mg [(ONOO)^{tBu}Y(bdsa)(THF)] (24.9 μmol, 1.0 eq., 19.94 mg) or in situ prepared 24.9 μmol of [(ONOO)^{tBu}Y(iPrO)(THF)] in 0.5 mL of toluene (preparation as for the homopolymerization), was added in one portion to the monomer solution. The reaction mixture was stirred at 60 °C in a heating block for the given time. Then, an aliquot of 0.05 mL was taken and quenched with 0.4 mL of wet CDCl₃. The respective amount of DHC was added by a syringe, the weight difference of the syringe before and after adding DHC determined the added amount. The mixture was further stirred at 60 °C for the given time. Another aliquot of 0.05 mL was taken and quenched. Conversions, relative molar masses, and polydispersities of the aliquots were determined by ¹H NMR spectroscopy and SEC measurements in chloroform. The polymerization mixture was dissolved in 1.5 mL chloroform and precipitated from methanol, filtered and dried. The purified PPDL-*b*-PDHC polymer was isolated in a quantitative yield and used for further analysis.

Block Copolymerization of Dihydrocarvide and β-Butyrolactone:

Block copolymers were synthesized via the sequential addition of monomers. The respective amount of dihydrocarvide was weighed and stirred in a heating block at 60 °C. The catalyst solution of 19.94 mg [(ONOO)^{tBu}Y(bdsa)(THF)] (24.9 μmol, 1.0 eq., 19.94 mg) or in situ prepared 24.9 μmol of [(ONOO)^{tBu}Y(iPrO)(THF)] in 0.5 mL of toluene (preparation as for the homopolymerization), was added in one portion. The reaction mixture was stirred in a heating block at 60 °C for 2 hours. An aliquot of 0.05 mL was taken and quenched with 0.4 mL wet CDCl₃. The respective amount of β-butyrolactone was added in one shot with a

syringe. The added amount of BBL was measured by weighing the syringe before and after addition. The reaction mixture was further stirred at 60 °C for the given time. The second aliquot of 0.05 mL was taken and quenched with 0.4 mL wet CDCl₃. Conversions, relative molar masses, and polydispersities of the aliquots were determined by ¹H NMR spectroscopy and SEC measurements in chloroform. The polymerization mixture was precipitated from methanol. The supernatant was decanted off and the polymer residue was dried under vacuum (60 °C, 200 mbar) overnight. After drying, the purified PDHC-*b*-PHB polymer was isolated in quantitative yield and used for further analysis.

SARA ATRP of Ethyl Acrylate with Ethyl α -bromoisobutyrate Initiator:

Under inert atmosphere, ethyl α -bromoisobutyrate (EBiB) (108 μ mol, 1 eq., 38.88 mg) and ethyl acrylate (1080 μ mol, 10 eq., 108.13 mg) were dissolved in 0.5 mL anhydrous and degassed dmf. A solution of copper(II) bromide (5.4 μ mol, 0.05 eq., 1.1 mg) and tris(2-dimethylaminoethyl)amine (19.4 μ mol, 0.18 eq., 4.82 μ L) in 0.5 mL dmf was added. To start the reaction, a cleaned Cu(0)-wire (2.5 cm) wrapped around a magnetic stir bar was inserted. The reaction was stirred at room temperature for 4 hours. An aliquot was taken for analysis using ¹H NMR spectroscopy. The remaining reaction mixture was filtered through aluminum oxide, rinsed with thf, and precipitated into a mixture of cold demineralized water and methanol (1:1). The sample was centrifuged, the supernatant removed, and the residue was dried under vacuum (60 °C, 200 mbar) overnight. The resulting PEA polymer was isolated in quantitative yield as a greenish and sticky solid and was analyzed by NMR spectroscopy and SEC in chloroform.

“Grafting from” Syntheses:

Synthesis of PDHC-2ME-OH via Thiol-ene Reaction:

PDHC was synthesized following the homopolymerization procedure for dihydrocarvide. For higher molecular weight polymers, [(ONOO)^tBuY(bdsa)(THF)] catalyst was used. PDHC was precipitated, dried, and subsequently analyzed before being redissolved for the thiol-ene reaction. Low-molecular weight PDHC (Table 1, Entry 11) was synthesized using [(ONOO)^tBuY(bdsa)(THF)] catalyst and 5 equivalents of isopropanol. An aliquot was taken for analysis (NMR spectroscopy and SEC), while the remaining reaction mixture was directly used for thiol-ene reaction.

For the thiol-ene reaction, PDHC (2.49 mmol monomer content, 1 eq.) was dissolved in 5 mL chloroform. 2,2-Dimethoxy-2-phenylacetophenone (0.50 mmol, 0.2 eq., 128.14 mg) and 2-mercaptoethanol (7.47 mmol, 3 eq., 585.98 mg, 532.7 μ L) were added and dissolved. The mixture was degassed with argon for 30 minutes. Then, the vial was placed in a light chamber equipped with a magnetic stirrer and a *Philips* TUV PL-S 9 W mercury lamp. The reaction mixture was stirred and irradiated overnight. Afterwards, the solvent was removed under vacuum, and the residue was dissolved in 2 mL thf before being precipitated into 40 mL of cold demineralized water. The sample was centrifuged, the supernatant removed, and the product dried under vacuum (60 °C and 200 mbar) overnight. The final product was obtained as a yellowish, sticky oil. The product PDHC-2ME-OH, isolated in quantitative yield, was characterized by elemental analysis, NMR spectroscopy and SEC in chloroform.

¹H NMR (700 MHz, CDCl₃, 296 K): δ [ppm] (per repeating unit) = 4.88 (tt, *J* = 9.0, 4.4 Hz, 1H), 3.71 (p, *J* = 6.3 Hz, 2H), 3.16 – 2.84 (m, 1H), 2.69 (h, *J* = 7.9, 7.2 Hz, 2H), 2.62 – 2.31 (m, 2H), 2.32 – 1.97 (m, 3H), 1.88 – 1.73 (m, 1H), 1.68 – 1.43 (m, 2H), 1.36 – 1.09 (m, 5H), 0.92 (dd, *J* = 14.1, 6.9 Hz, 3H).

Elemental Analysis of PDHC-2ME-OH:

	Calculated [%]	Found [%]
C	58.50	58.41
H	9.00	8.96

Synthesis of PDHC-2ME-Br Macroinitiator:

PDHC-2ME-OH (2.49 mmol, 1 eq., 613.64 mg) was dissolved in 10 mL dichloromethane and triethylamine (7.47 mmol, 3 eq., 755.89 mg, 1.04 mL) was added. The solution was degassed using argon for 30 minutes. 2-Bromoisobutyryl bromide (7.47 mmol, 3 eq., 1717.35 mg, 741.2 μL) was added, and the reaction mixture was stirred overnight. The precipitate was filtered, and the filtrate was washed with a saturated sodium hydrogen carbonate solution. The solvent of the organic phase was removed under vacuum and the residue was redissolved in thf. The solution was dialyzed against thf using a Spectra/Por® 7 dialysis membrane with a molecular weight cut-off of 1 kDa. Dialysis was carried out for 4 days, with the thf being replaced after 1, 2, 20, 44 and 68 h. After dialysis, thf inside the membrane was removed under vacuum and the residue was freeze-dried from benzene. PDHC-2ME-Br was isolated in quantitative yield as a brown, sticky oil and was analyzed via elemental analysis, NMR spectroscopy and SEC.

¹H NMR (400 MHz, CDCl₃, 298 K): δ [ppm] (per repeating unit) = 4.87 (s, 1H), 4.30 (t, *J* = 6.9 Hz, 2H), 2.77 (q, *J* = 6.8, 6.4 Hz, 2H), 2.71 – 2.35 (m, 2H), 2.32 – 2.20 (m, 1H), 2.14 – 1.98 (m, 2H), 1.94 (s, 6H), 1.84 – 1.75 (m, 1H), 1.74 – 1.40 (m, 2H), 1.40 – 1.28 (m, 2H), 1.20 (d, *J* = 5.5 Hz, 3H), 1.03 – 0.80 (m, 3H).

Elemental Analysis of PDHC-2ME-Br:

	Calculated [%]	Found [%]
C	48.61	48.17
H	6.88	6.77

SARA ATRP of Ethyl Acrylate (10 eq.) with PDHC-2ME-Br Macroinitiator:

Under inert atmosphere, PDHC-2ME-Br (108 μmol, 1 eq., 42.7 mg) and ethyl acrylate (1080 μmol, 10 eq., 108.1 mg) were dissolved in 0.5 mL dmf. A solution of copper(II) bromide (5.4 μmol, 0.05 eq., 1.1 mg) and tris(2-dimethylaminoethyl)amine (19.4 μmol, 0.18 eq., 4.82 μL) in 0.5 mL dmf was added. To start the reaction a cleaned Cu(0)-wire (2.5 cm) wrapped around a magnetic stir bar was inserted, and the reaction was stirred at room temperature for 4 hours. An aliquot was taken for analysis using ¹H NMR spectroscopy and SEC in chloroform. The remaining reaction mixture was filtered through aluminum oxide, rinsed with thf, and precipitated into cold demineralized water. The sample was centrifuged, the supernatant removed, and the residue freeze-dried from benzene. PDHC-g-PEA polymer was isolated in quantitative yield as a brown and sticky oil and was analyzed by NMR spectroscopy and SEC. SARA ATRP of ethyl acrylate (15 eq.) was performed in the same way.

ARGET ATRP of Ethyl Acrylate (10 eq.) with PDHC-2ME-Br Macroinitiator:

PDHC-2ME-Br (110 μmol , 1 eq., 43.5 mg) was dissolved in 0.5 mL dmf. In a separate vial, copper(II) bromide (19.8 μmol , 0.18 eq., 4.42 mg) and tris[(4-dimethylaminopyridyl)methyl]amine (19.8 μmol , 0.18 eq., 8.31 mg) were dissolved in 0.5 mL dmf and mixed until the solution turned yellow. Then, silver(0) powder (39.6 μmol , 0.36 eq., 4.27 mg) and ethyl acrylate (1100 μmol , 10 eq., 110.1 mg) were added and the solution was preheated in a heating block at 50 °C. The macroinitiator solution was added to this mixture to initiate the reaction, which was stirred at 50 °C for 3 hours. An aliquot was taken and analyzed by NMR spectroscopy and SEC in chloroform. The remaining solution was filtered through aluminum oxide, rinsed with thf, and precipitated into cold demineralized water. The sample was centrifuged, the supernatant removed, and the residue freeze-dried from benzene. The final brownish PDHC-*g*-PEA polymer was isolated in quantitative yield and analyzed using NMR techniques and SEC in chloroform. ARGET ATRP of ethyl acrylate (15 eq.) was performed in the same way.

2. Results

2.1 Synthesis of Dihydrocarvide

Analysis of Dihydrocarvone

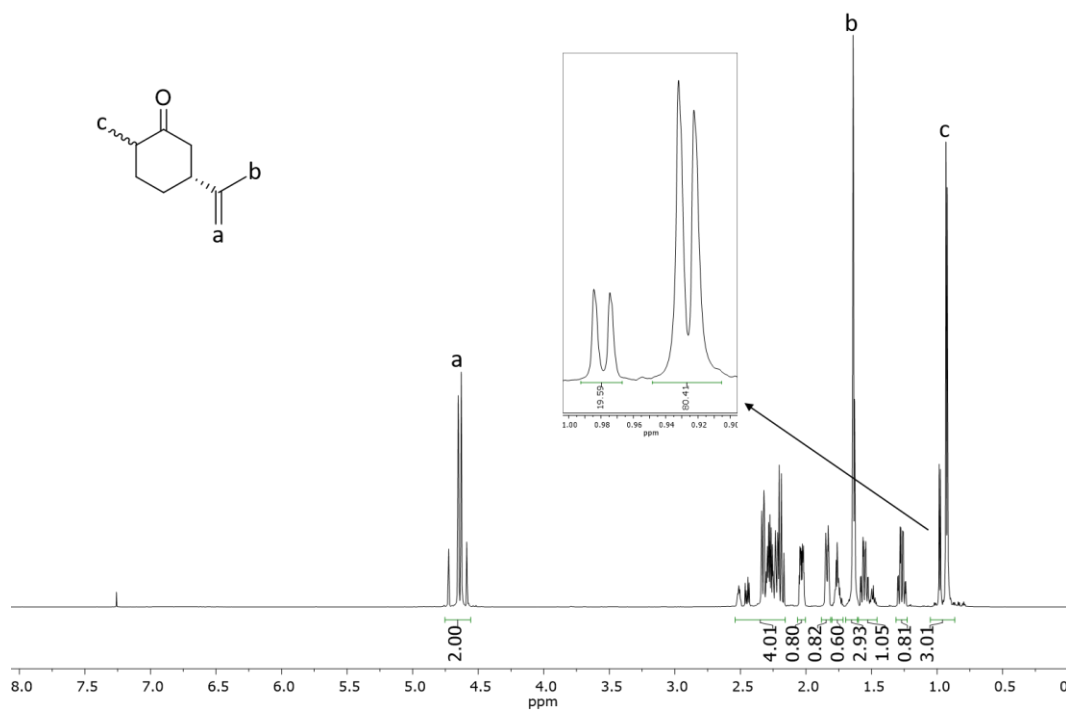


Figure S1: ¹H NMR spectrum of (+)-dihydrocarvone as received (*Sigma-Aldrich*, batch number: SHBL6822; CDCl₃, 700 MHz).

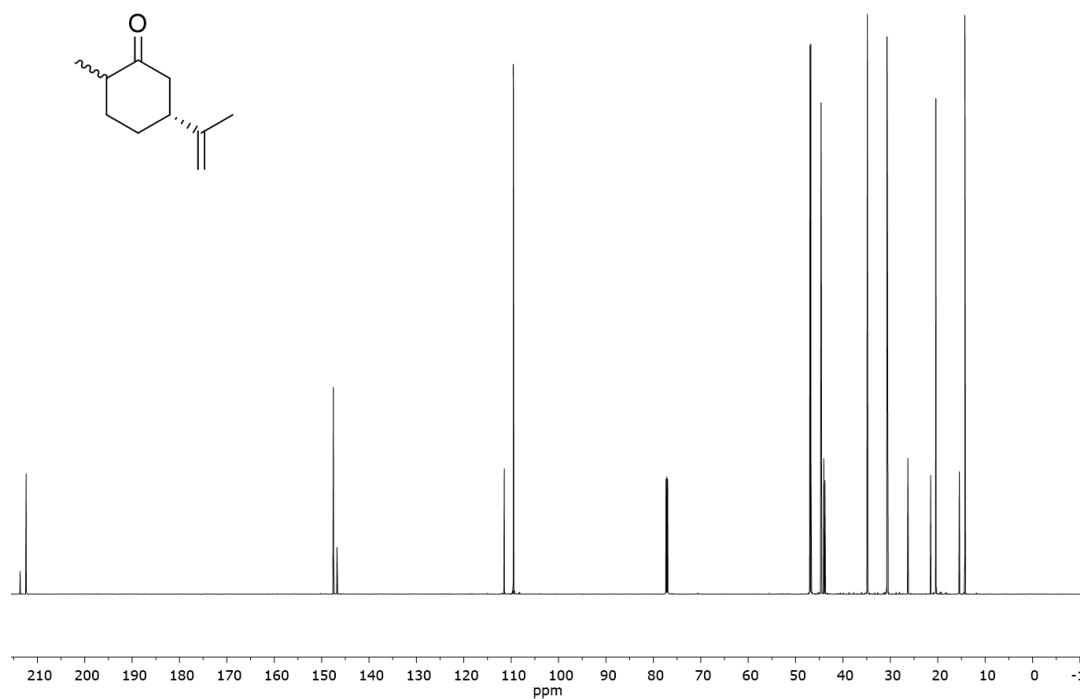


Figure S2: ¹³C NMR spectrum of (+)-dihydrocarvone as received (CDCl₃, 176 MHz).

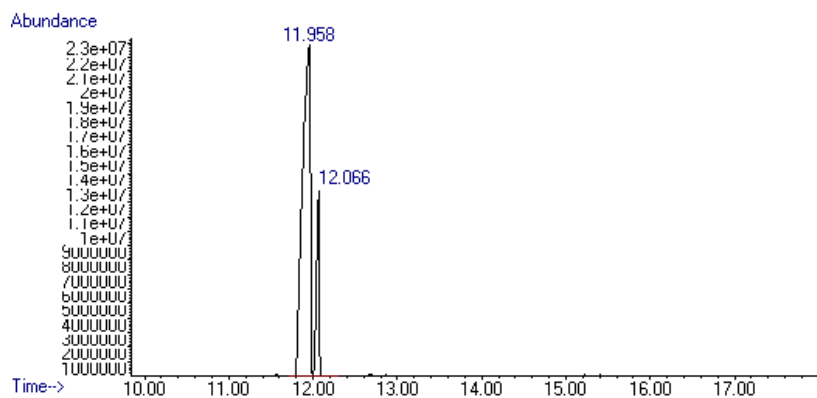


Figure S3: Chromatogram of abundance over time for the GC-MS measurement of dihydrocarvone (peak area = 83:17).

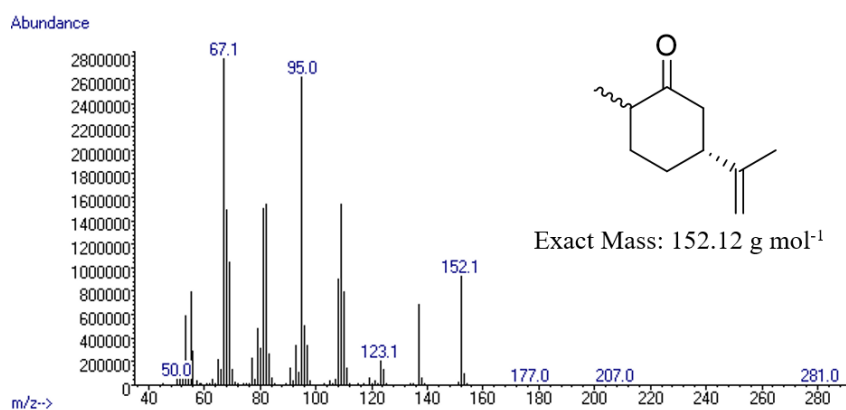


Figure S4: Mass spectrum of the dihydrocarvone GC-MS analysis (11.958 min).

NMR Spectroscopy of Dihydrocarvide

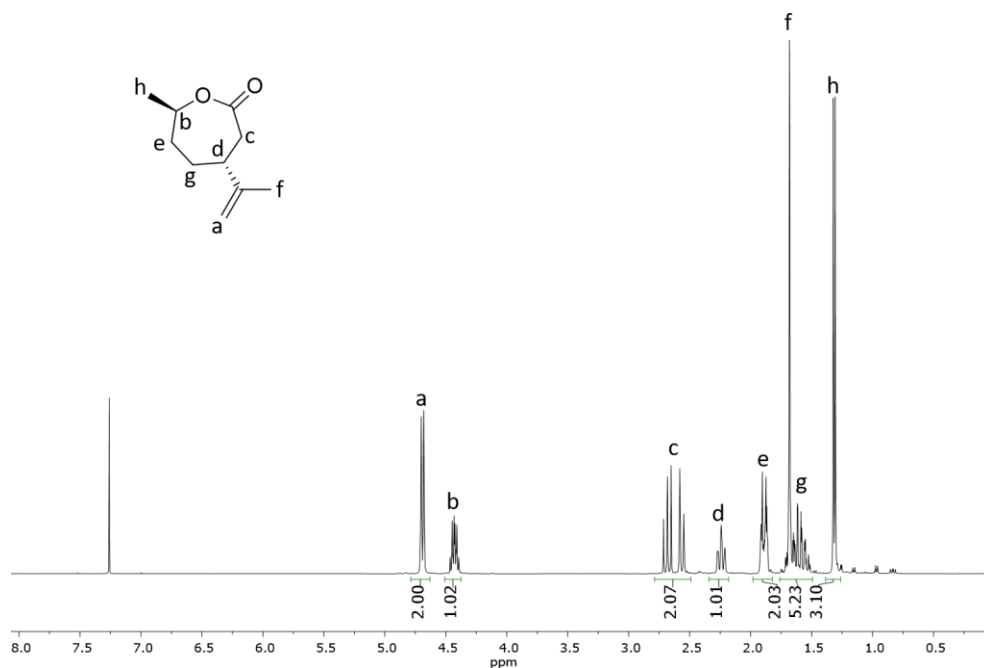


Figure S5: ^1H NMR spectrum of dihydrocarvide after Bayer-Villiger oxidation, column chromatography, and distillation (CDCl_3 , 400 MHz).

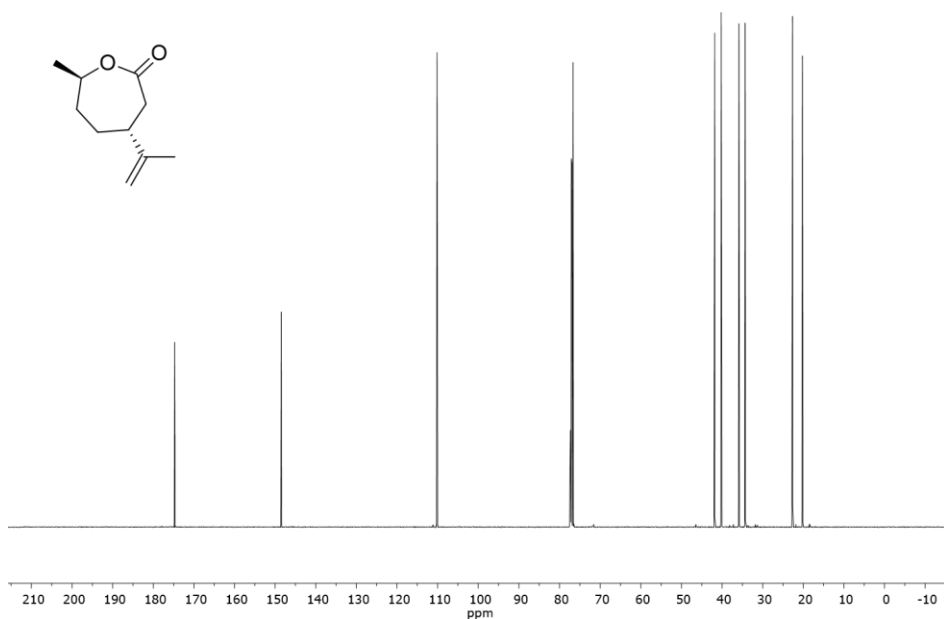


Figure S6: ^{13}C NMR spectrum of dihydrocarvide after Bayer-Villiger oxidation, column chromatography, and distillation (CDCl_3 , 176 MHz).

GC-MS of Dihydrocarvide

Abundance

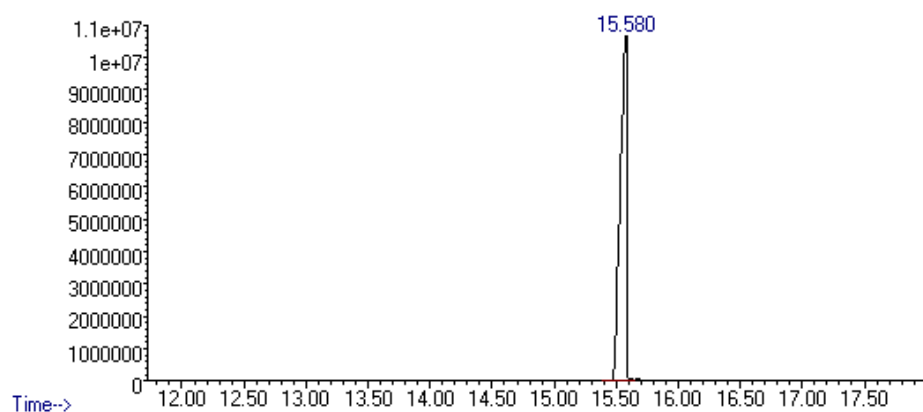


Figure S7: Chromatogram of abundance over time for the GC-MS measurement of dihydrocarvide.

Abundance

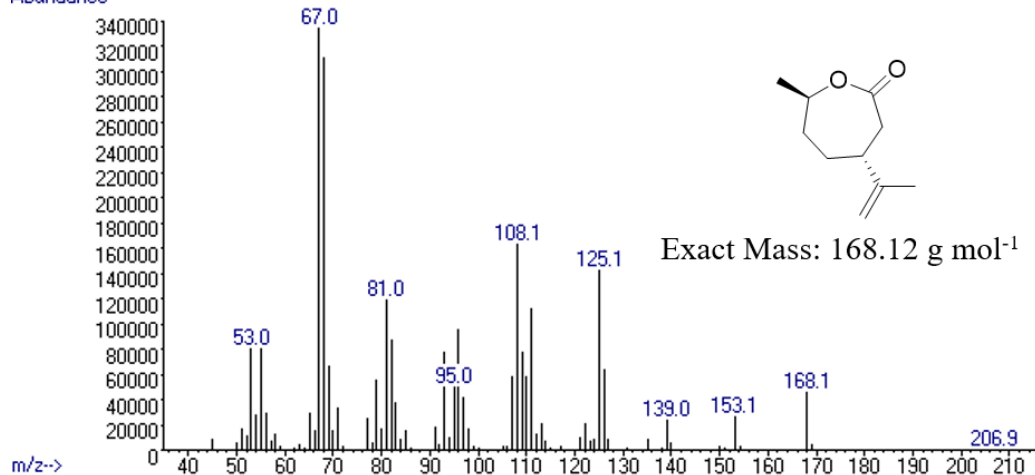
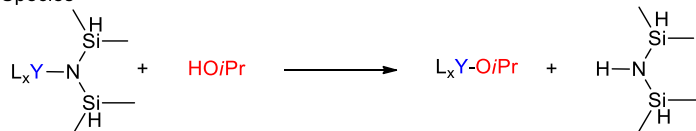


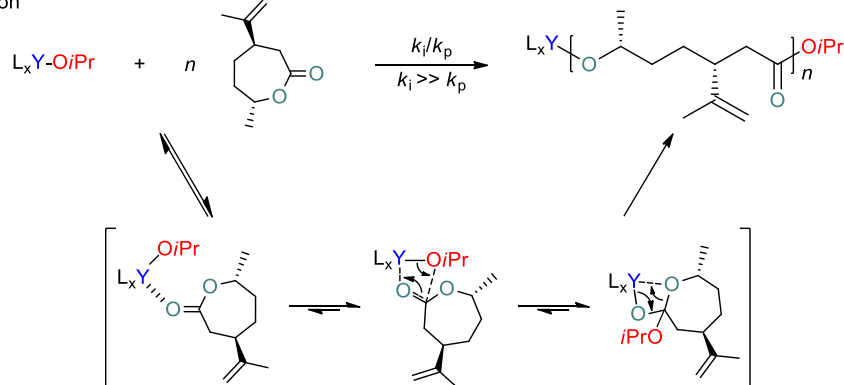
Figure S8: Mass spectrum of the dihydrocarvide GC-MS analysis (15.580 min).

2.2 Homopolymerization of Dihydrocarvide

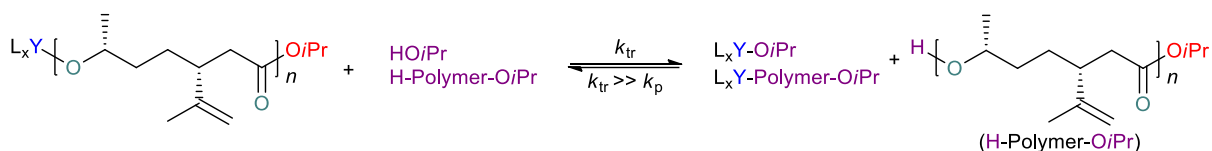
Generation of Active Species



Initiation & Propagation



Transfer Reactions



Scheme S1: Mechanism of the coordination-insertion ring-opening polymerization, k are rate constants for initiation (k_i), propagation (k_p), and reversible transfer reactions (k_{tr}).

NMR Spectra of Poly(dihydrocarvide)

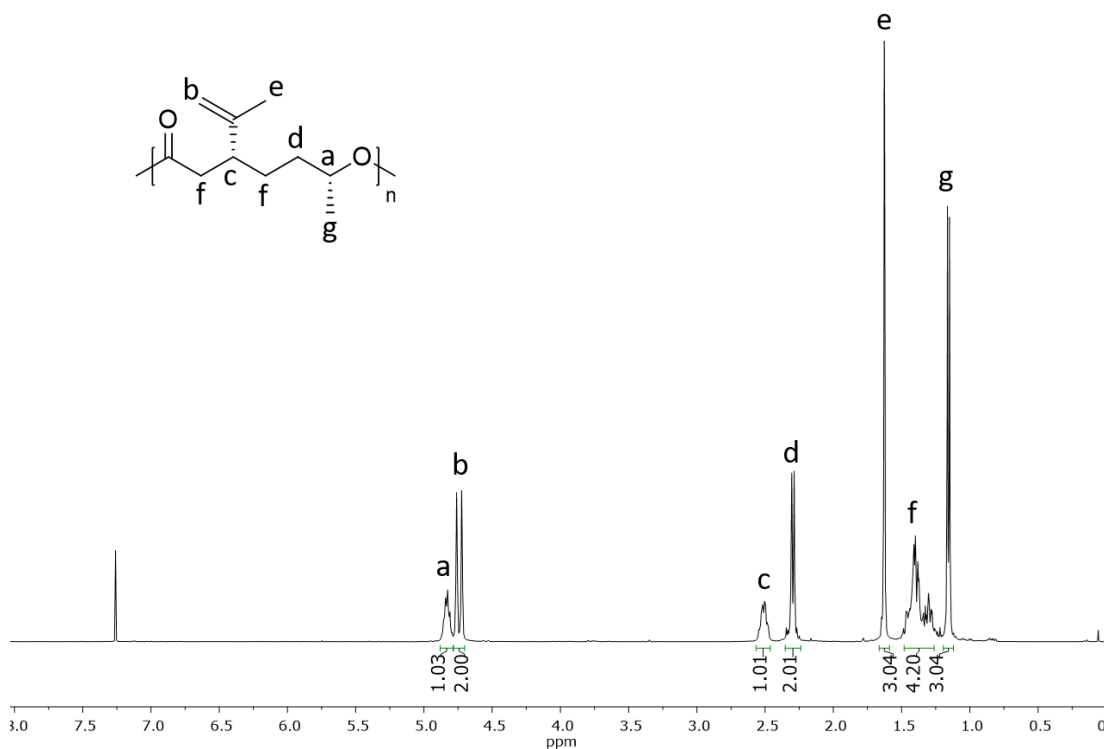


Figure S9: ^1H NMR spectrum of PDHC produced with $[(\text{ONOO})^{\text{tBu}}\text{Y}(\text{bdsa})(\text{THF})]$ catalyst after drying (Table 1, Entry 4, CDCl_3 , 400 MHz).

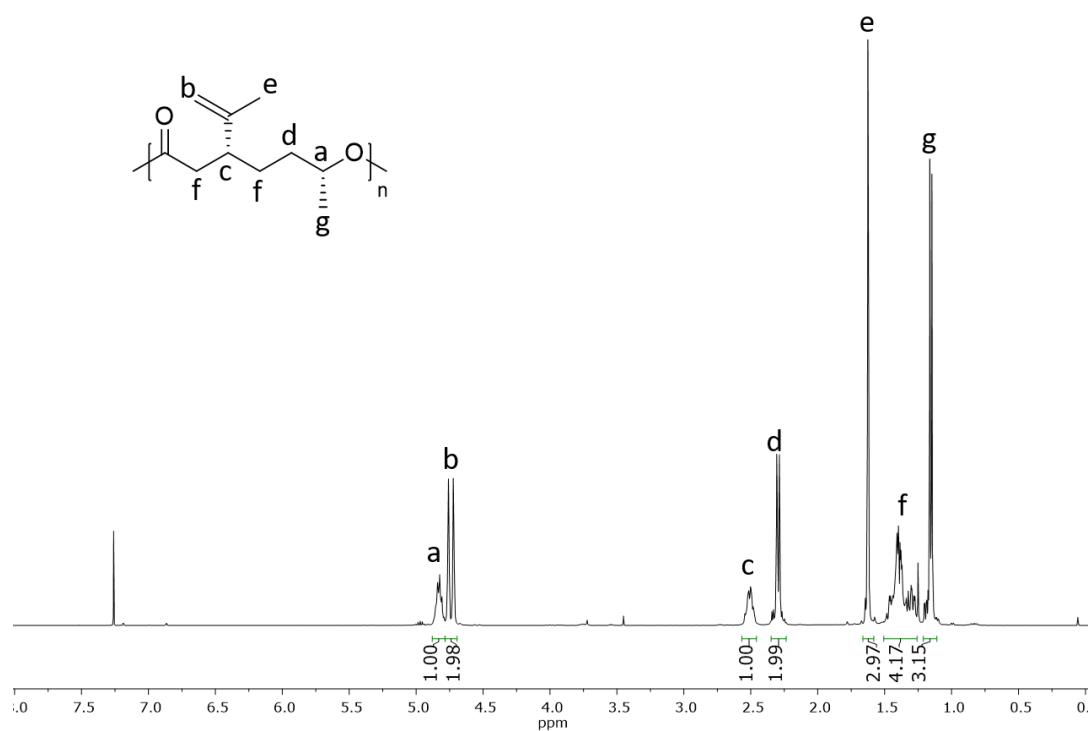


Figure S10: ¹H NMR spectrum of PDHC produced with [(ONOO)^tBuY(*i*PrO)(THF)] catalyst (Table 1, Entry 9, CDCl₃, 400 MHz).

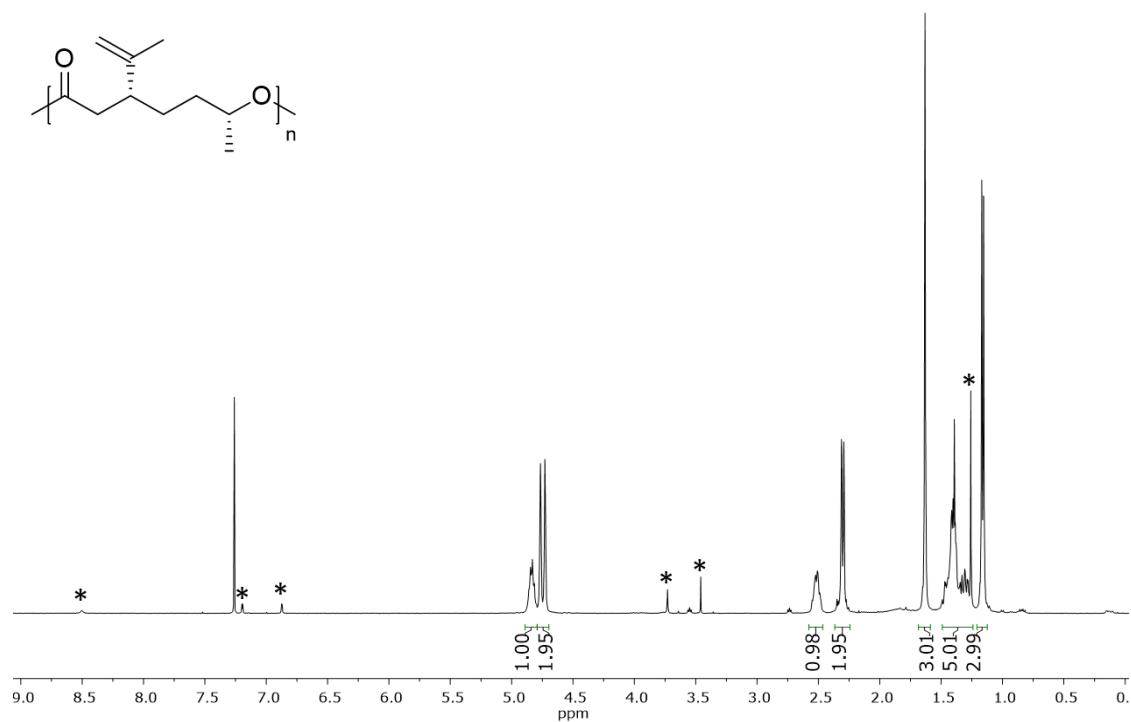


Figure S11: ¹H NMR spectrum of PDHC produced without solvent in a neat reaction (Table 1, Entry 5, CDCl₃, 400 MHz), catalyst/ligand residues are marked with *.

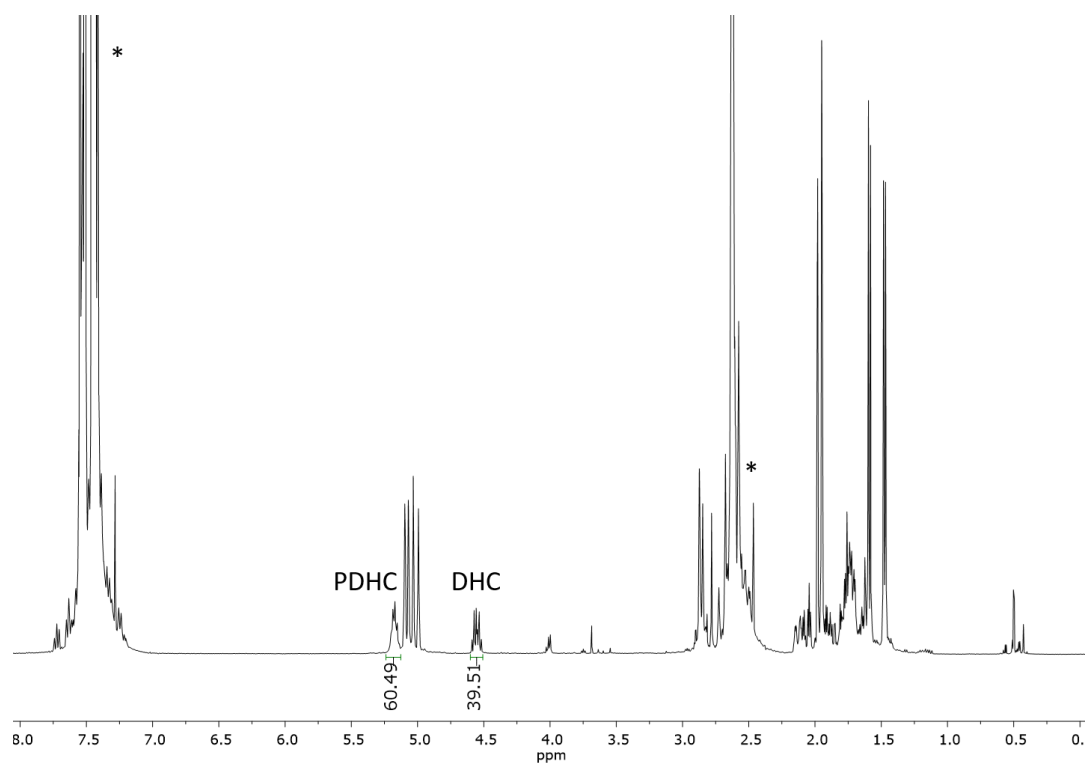


Figure S12: ^1H NMR spectrum of an aliquot with a DHC/PDHC mixture in toluene for conversion determination after 5 min of polymerization using the $[(\text{ONOO})^t\text{BuY}(\text{bdsa})(\text{THF})]$ catalyst at 60°C (Kinetic measurement Figure S18, CDCl_3 , 400 MHz). (* = solvent)

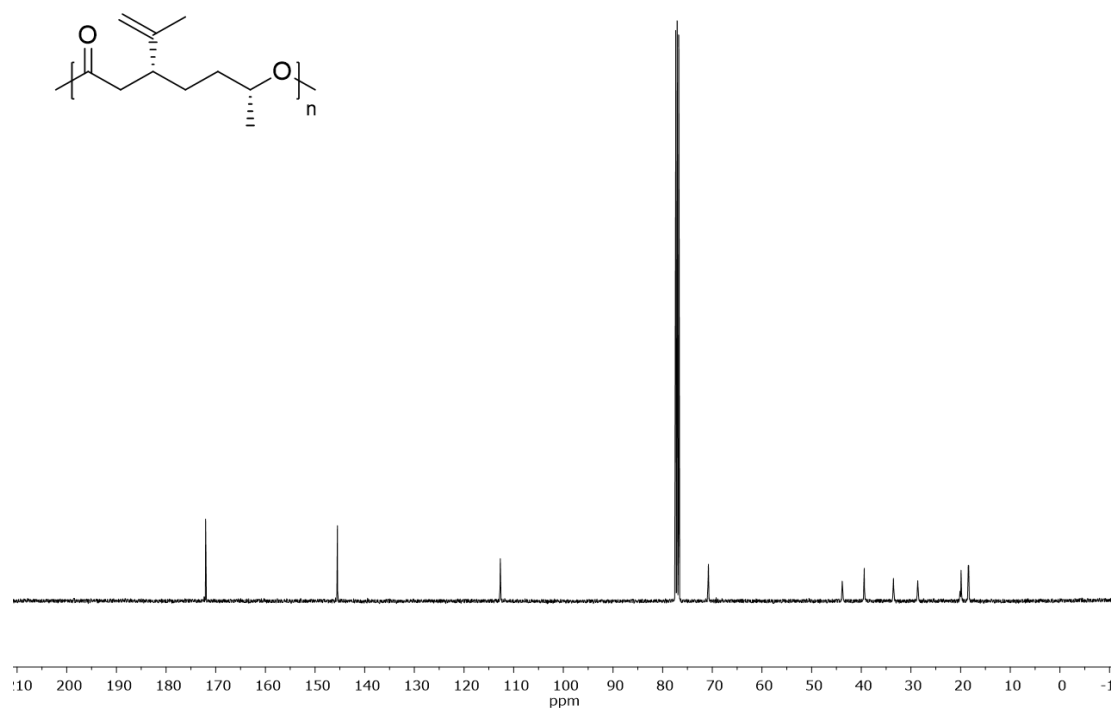


Figure S13: ^{13}C NMR spectrum of PDHC produced with $[(\text{ONOO})^t\text{BuY}(\text{bdsa})(\text{THF})]$ catalyst after drying (Table 1, Entry 7, CDCl_3 , 101 MHz).

Mass Spectrometry

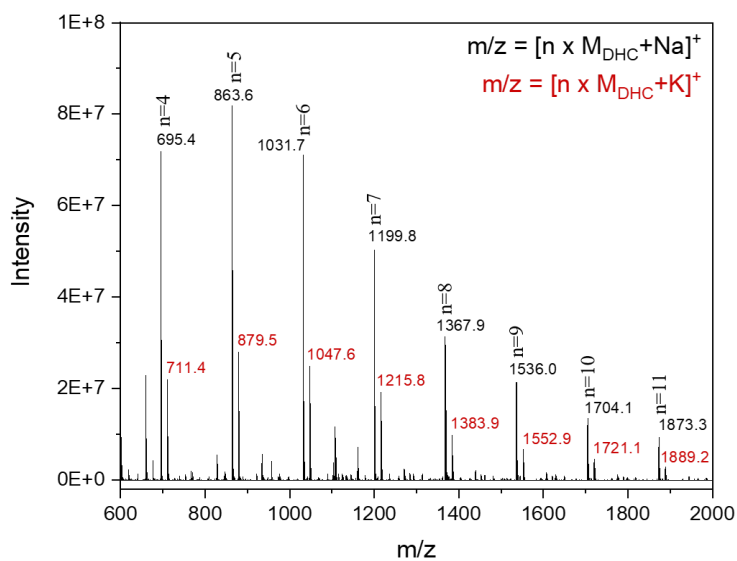


Figure S14: ESI-MS measurement in acetonitrile with $[(\text{ONOO})^{i\text{Bu}}\text{Y}(\text{bdsa})(\text{THF})]$ and DHC (4.98 μmol of catalyst, 24.9 μmol DHC, 1 mL toluene, RT).

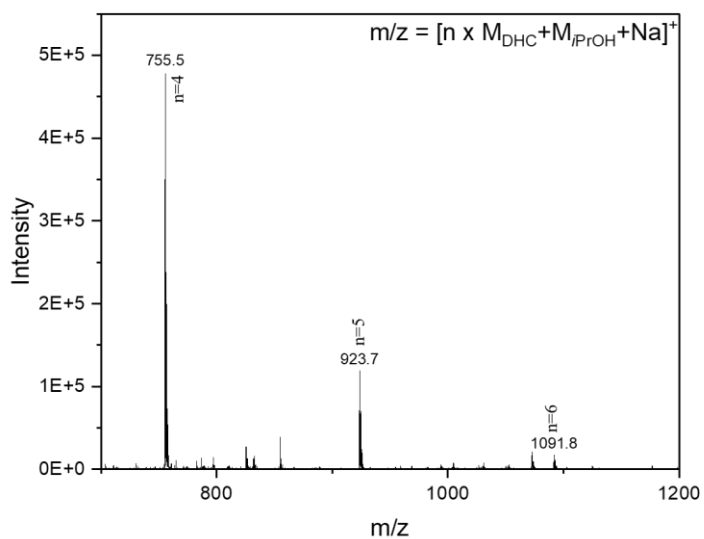


Figure S15: MALDI-TOF spectrum of DHC oligomerization in tetrahydrofuran with $[(\text{ONOO})^{i\text{Bu}}\text{Y}(\text{bdsa})(\text{THF})]$, $i\text{PrOH}$, and DHC (4.98 μmol catalyst, 4.98 μmol $i\text{PrOH}$, 39.84 μmol DHC, 1 mL thf, RT).

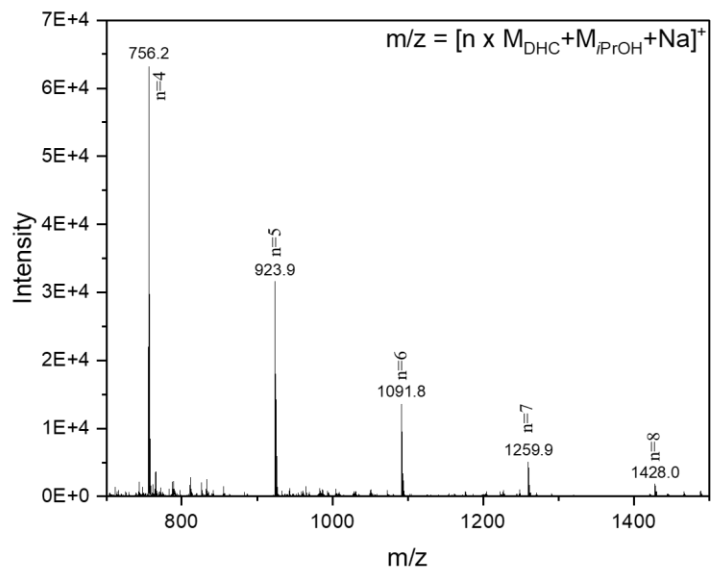


Figure S16: MALDI-TOF spectrum of DHC oligomerization in tetrahydrofuran with $[(\text{ONOO})^{i\text{Bu}}\text{Y}(\text{bdsa})(\text{THF})]$, *i*PrOH, and DHC (4.98 μmol catalyst, 4.98 μmol *i*PrOH, 39.84 μmol DHC, 1 mL thf, 60 °C).

Differential Scanning Calorimetry

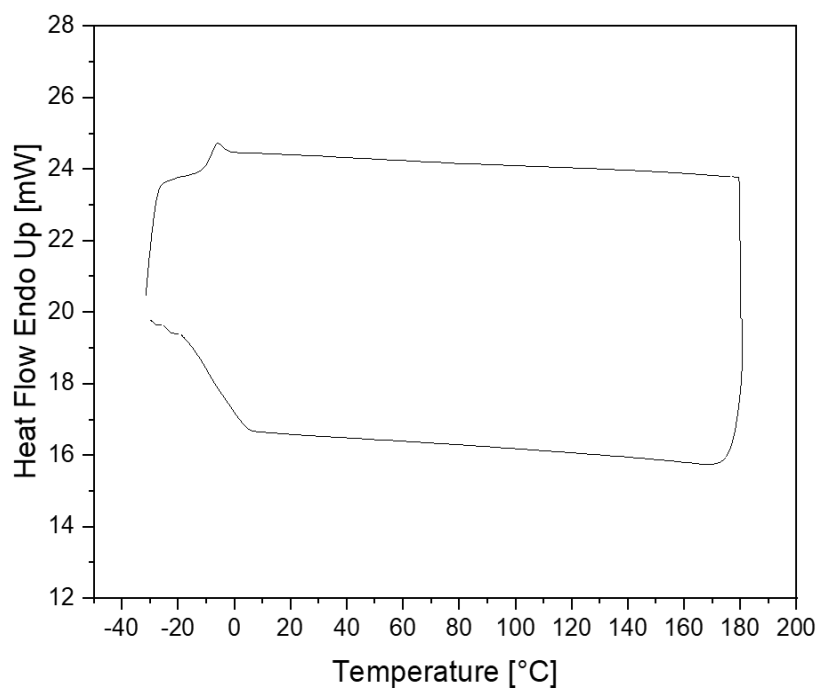


Figure S17: DSC analysis of PDHC with $T_g = -8$ °C (Table 1, Entry 7).

Polymerization Studies

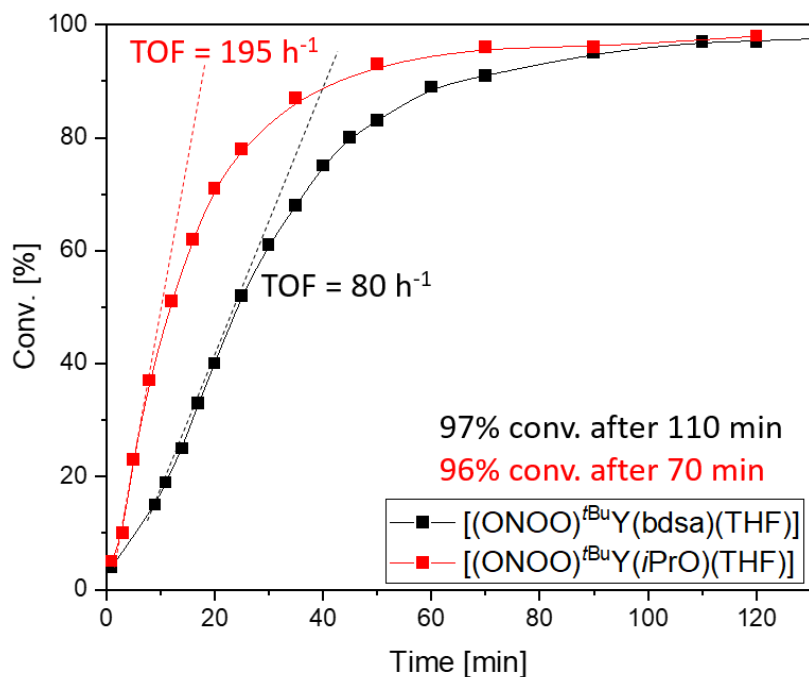


Figure S18: Polymerization study of dihydrocarvide polymerization at room temperature in toluene. The conversion was determined by ¹H NMR spectroscopy and is plotted against reaction time.

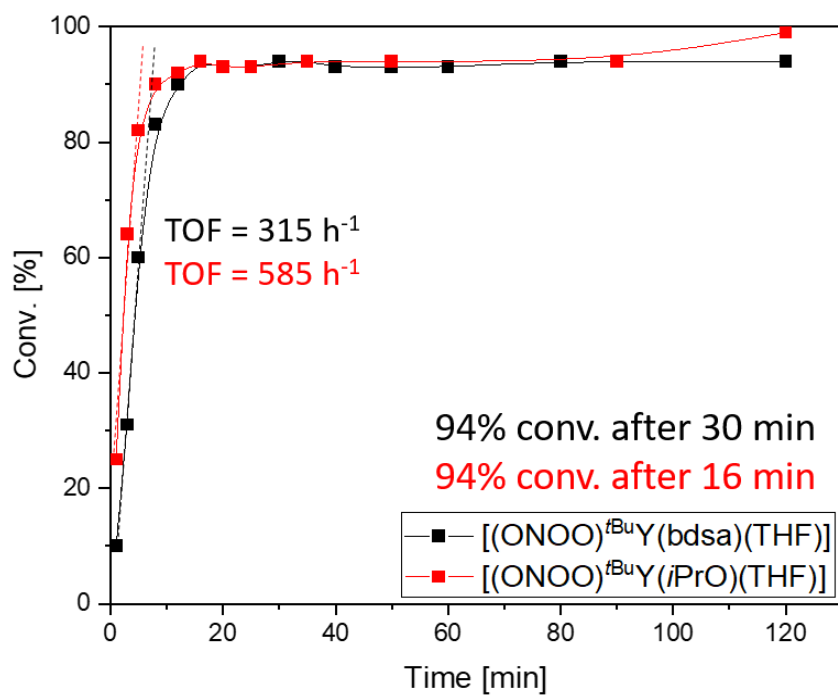


Figure S19: Polymerization study of dihydrocarvide polymerization 60 °C in toluene. The conversion was determined by ¹H NMR spectroscopy and is plotted against reaction time.

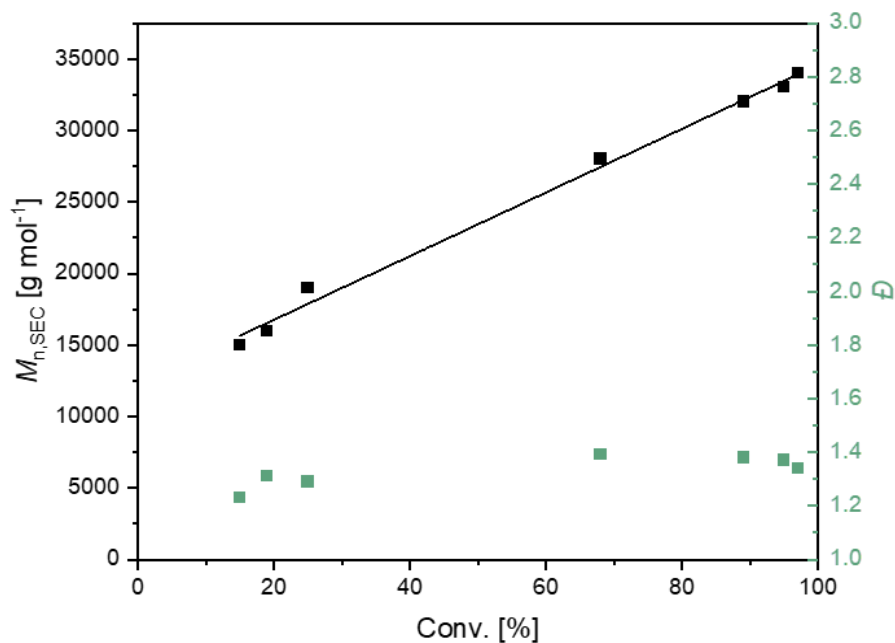


Figure S20: Dependency of number-average molar mass and polydispersity on the conversion for the kinetic measurement of DHC with [(ONOO)^tBuY(bdsa)(THF)] catalyst at room temperature.

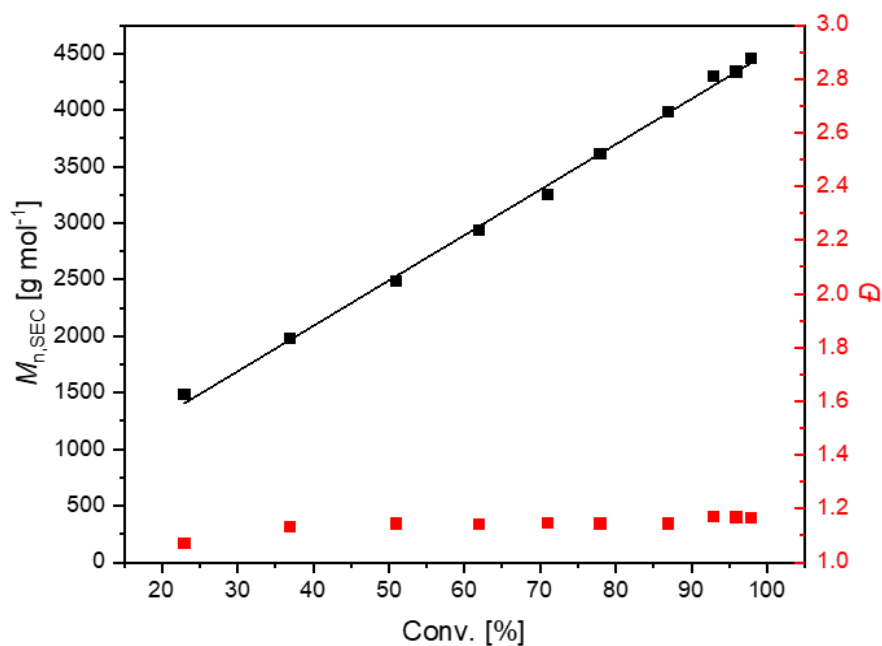


Figure S21: Dependency of number-average molar mass and polydispersity on the conversion for the kinetic measurement of DHC with [(ONOO)^tBuY(*i*PrO)(THF)] catalyst at room temperature.

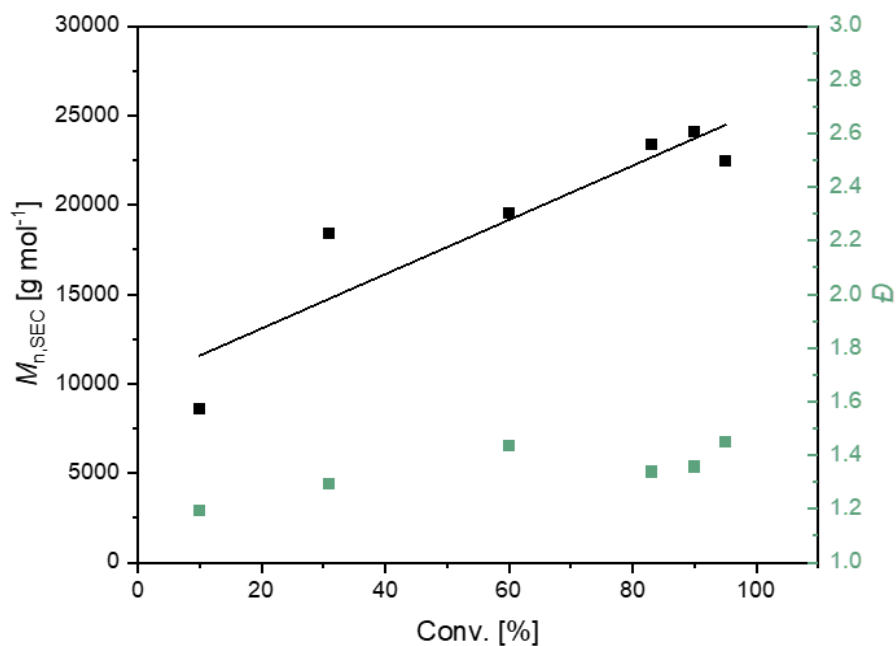


Figure S22: Dependency of number-average molar mass and polydispersity on the conversion for the kinetic measurement of DHC at 60 °C with [(ONOO)^tBuY(bdsa)(THF)] catalyst.

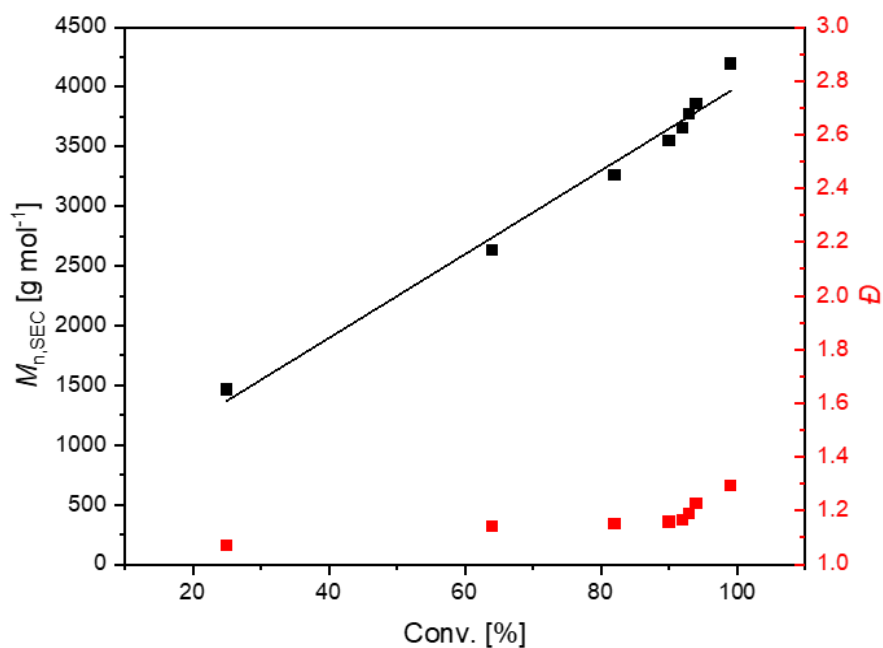


Figure S23: Dependency of number-average molar mass and polydispersity on the conversion for the kinetic measurement of DHC with [(ONOO)^tBuY(*i*PrO)(THF)] catalyst at 60 °C.

SEC Traces

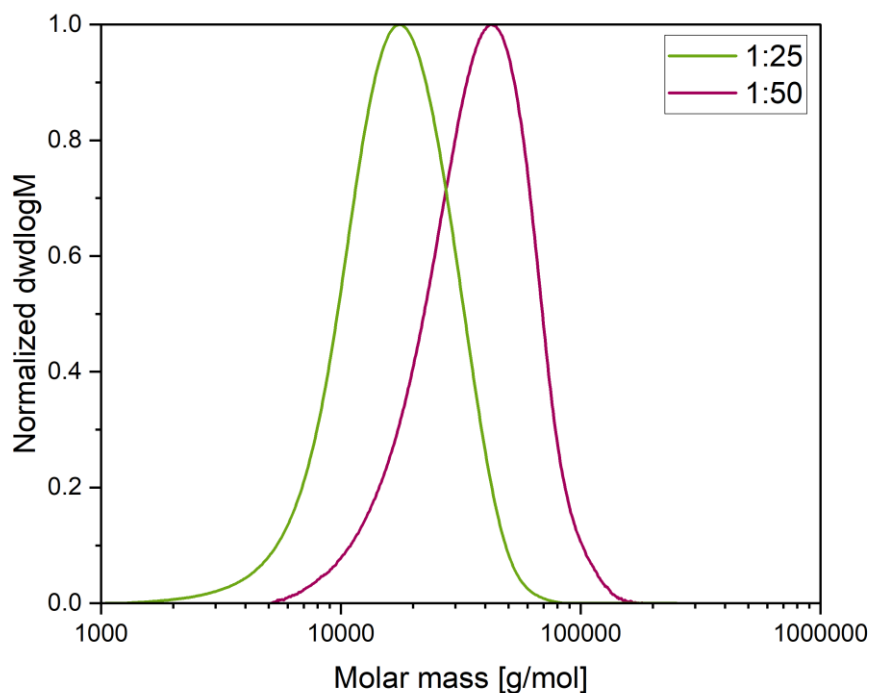


Figure S24: SEC traces of PDHC polymerized at 60 °C with [(ONOO)^tBuY(bdsa)(THF)] catalyst (catalyst:DHC; 1:25, 1:50) (Table 1, Entry 4 and 7).

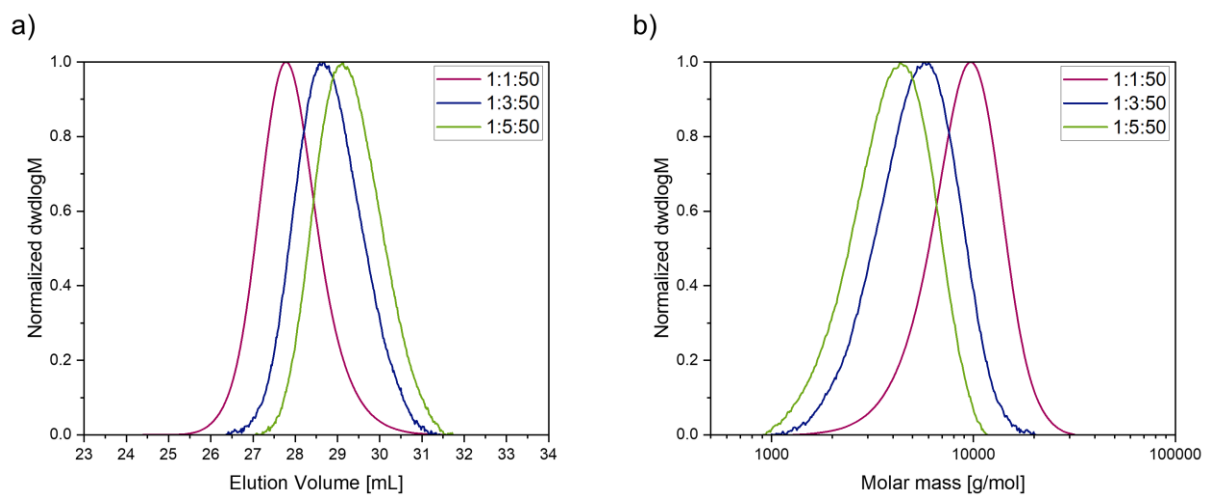


Figure S25: SEC traces of PDHC produced with [(ONOO)^tBuY(bdsa)(THF)] catalyst and different equivalents of *i*PrOH at 60 °C ([[(ONOO)^tBuY(bdsa)(THF)]:*i*PrOH:DHC; 1:1:50, 1:3:50, 1:5:50) (Table 1, Entry 9-11) as the normalized dwdlogM plotted against a) elution volume and b) corresponding molar mass.

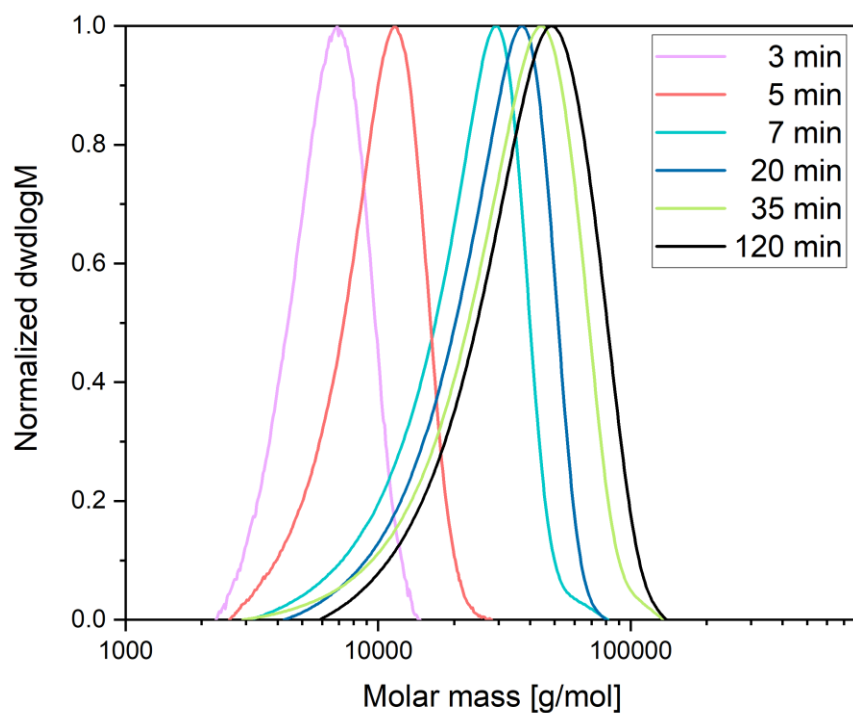


Figure S26: SEC traces from kinetic measurements of DHC polymerization at room temperature with $[(\text{ONOO})^{\text{tBuY}}(\text{bdsa})(\text{THF})]$ catalyst.

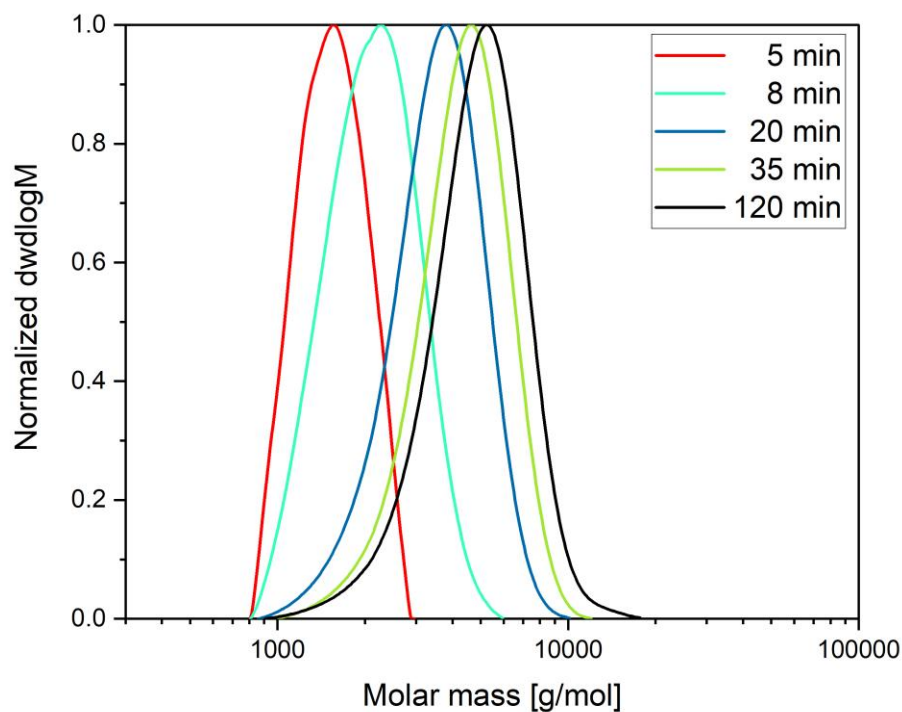


Figure S27: SEC traces from kinetic measurements of DHC polymerization with $[(\text{ONOO})^{\text{tBuY}}(\text{iPrO})(\text{THF})]$ catalyst at room temperature.

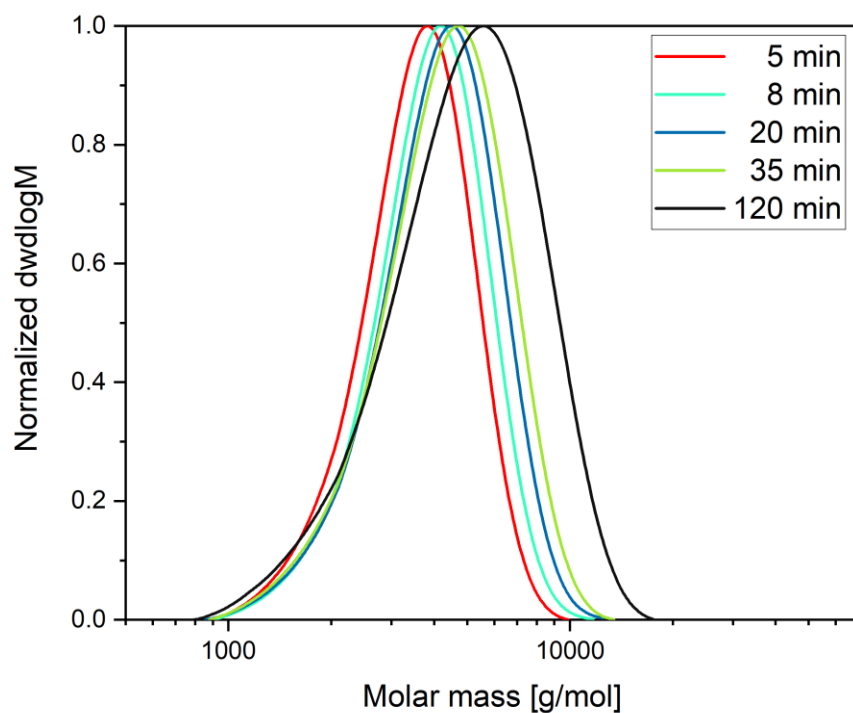


Figure S28: SEC traces from kinetic measurements of DHC polymerization with $[(\text{ONOO})^t\text{BuY}(\text{iPrO})(\text{THF})]$ catalyst at 60 °C.

2.3 Block Copolymerization

NMR Spectra of PPDL-*b*-PDHC Copolymers

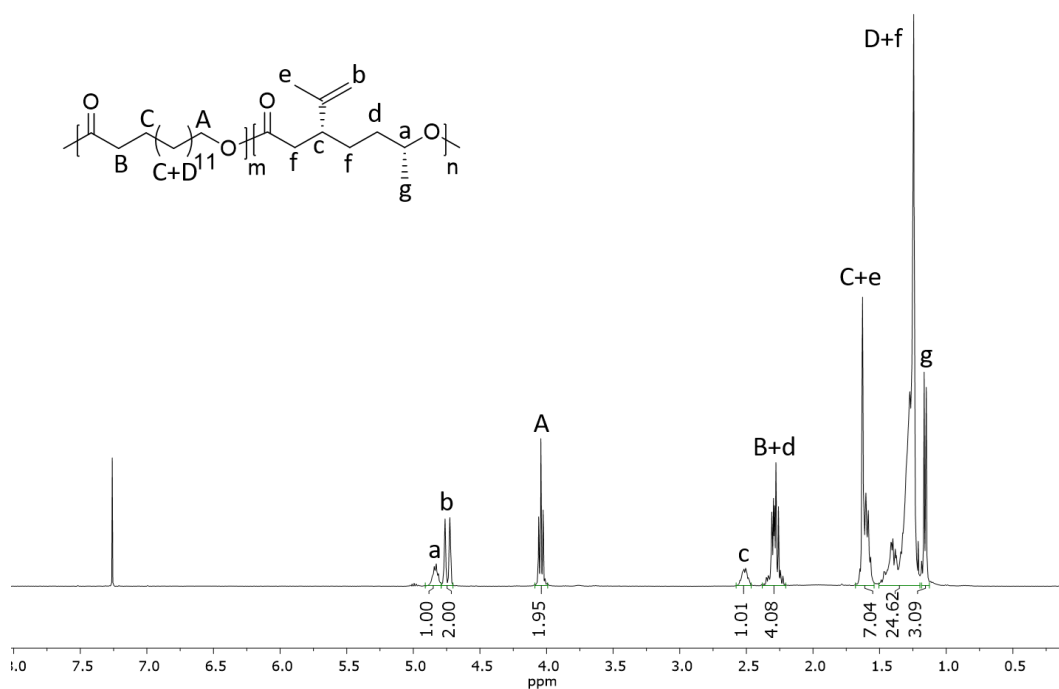


Figure S29: ^1H NMR spectrum of PPDL-*b*-PDHC copolymer (PPDL/PDHC = 50/50; Table 2, Entry 3, CDCl_3 , 400 MHz).

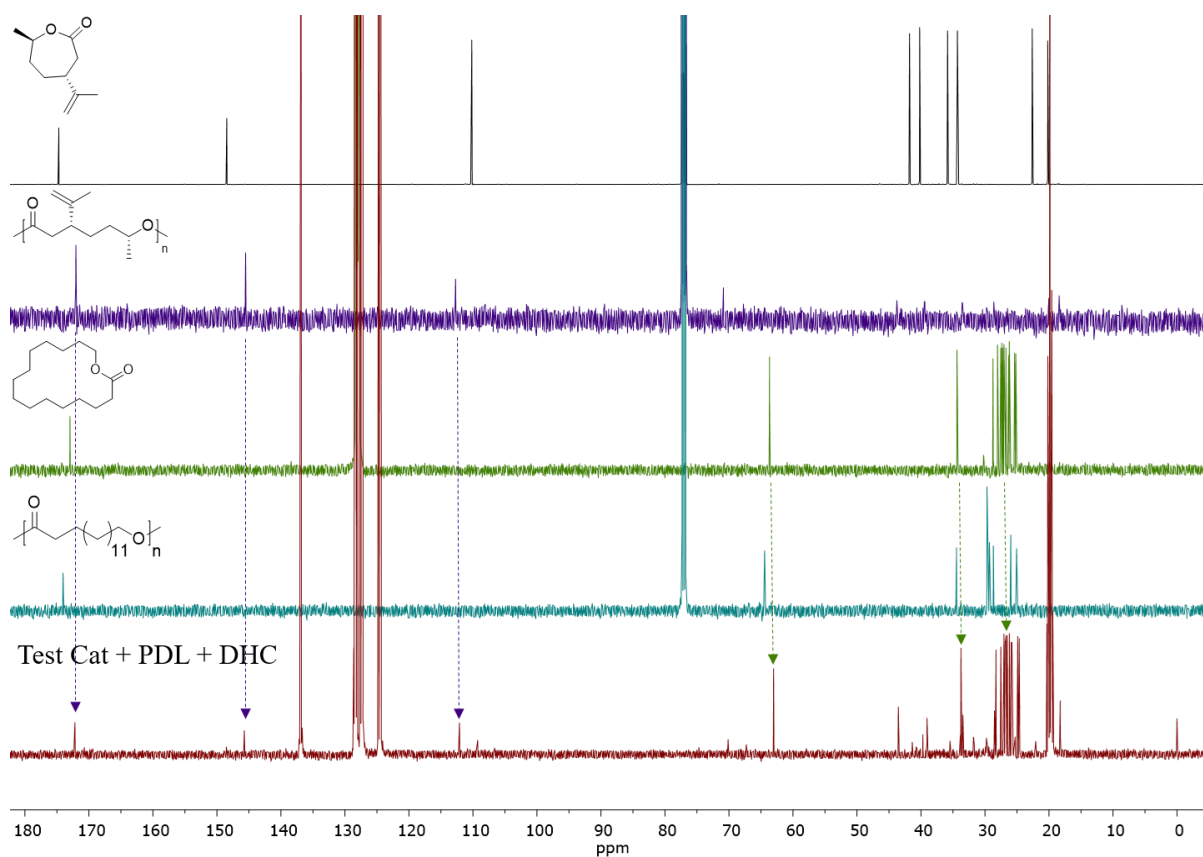


Figure S30: Stacked ^{13}C NMR spectra of DHC, PDHC, PDL, PPDL, and a test reaction of $[(\text{ONOO})^t\text{BuY}(\text{bdsa})(\text{THF})]$ catalyst with 10 equivalents of DHC and 10 equivalents of PDL (CDCl_3 , 126 MHz, 1024 scans).

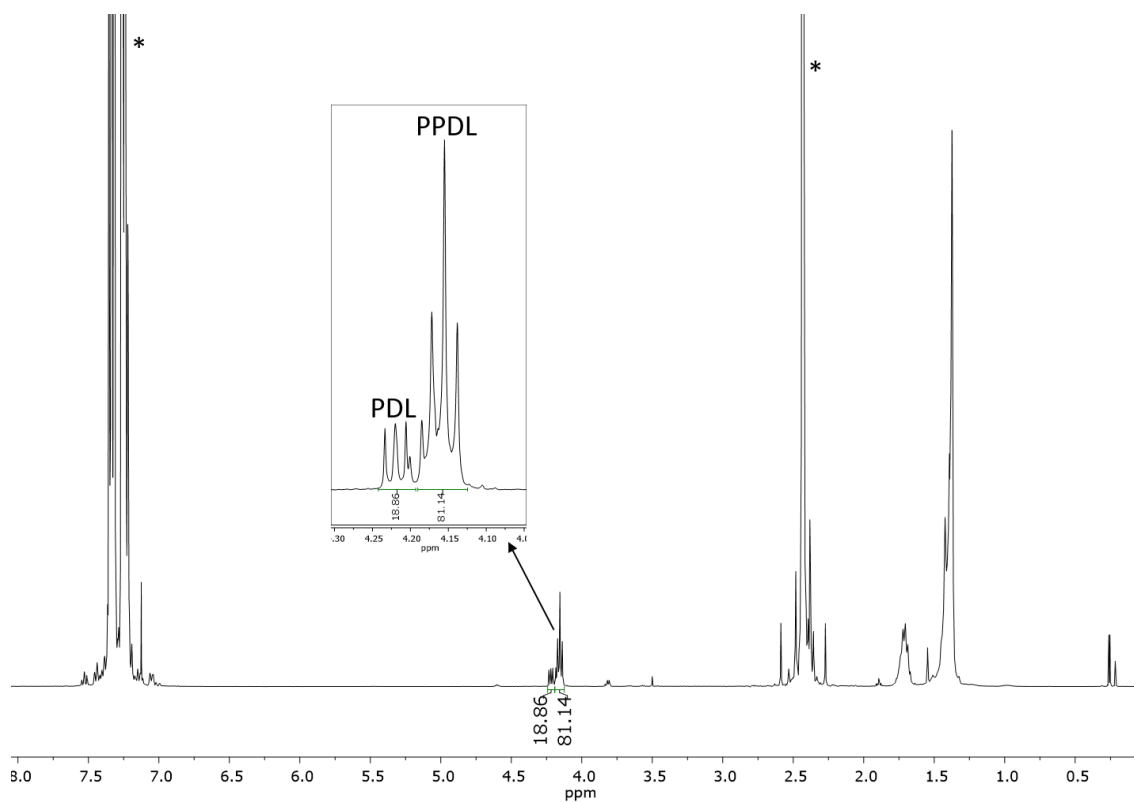


Figure S31: ^1H NMR spectrum of an aliquot of the first block with a PDL/PPDL mixture for conversion determination (Table 2, Entry 1, CDCl_3 , 400 MHz). (* = solvent)

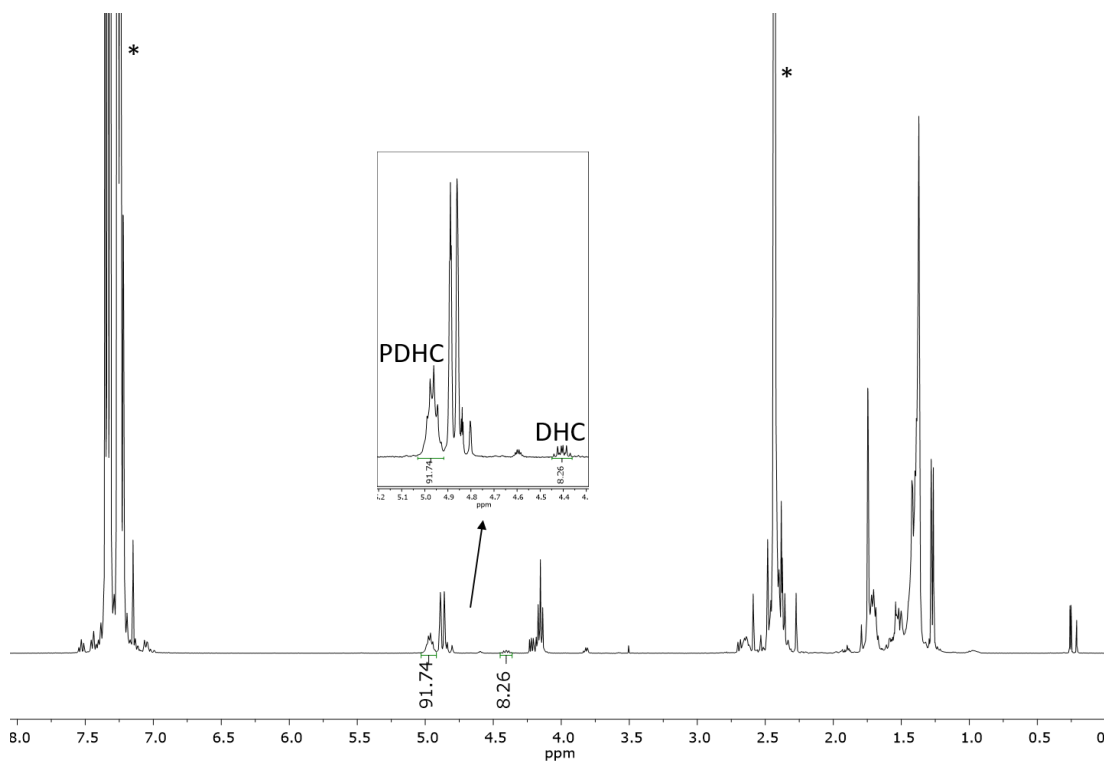


Figure S32: ^1H NMR spectrum of an aliquot of the second block with a PDL/PPDL and DHC/PDHC mixture for conversion determination of DHC (Table 2, Entry 1, CDCl_3 , 400 MHz). (* = solvent)

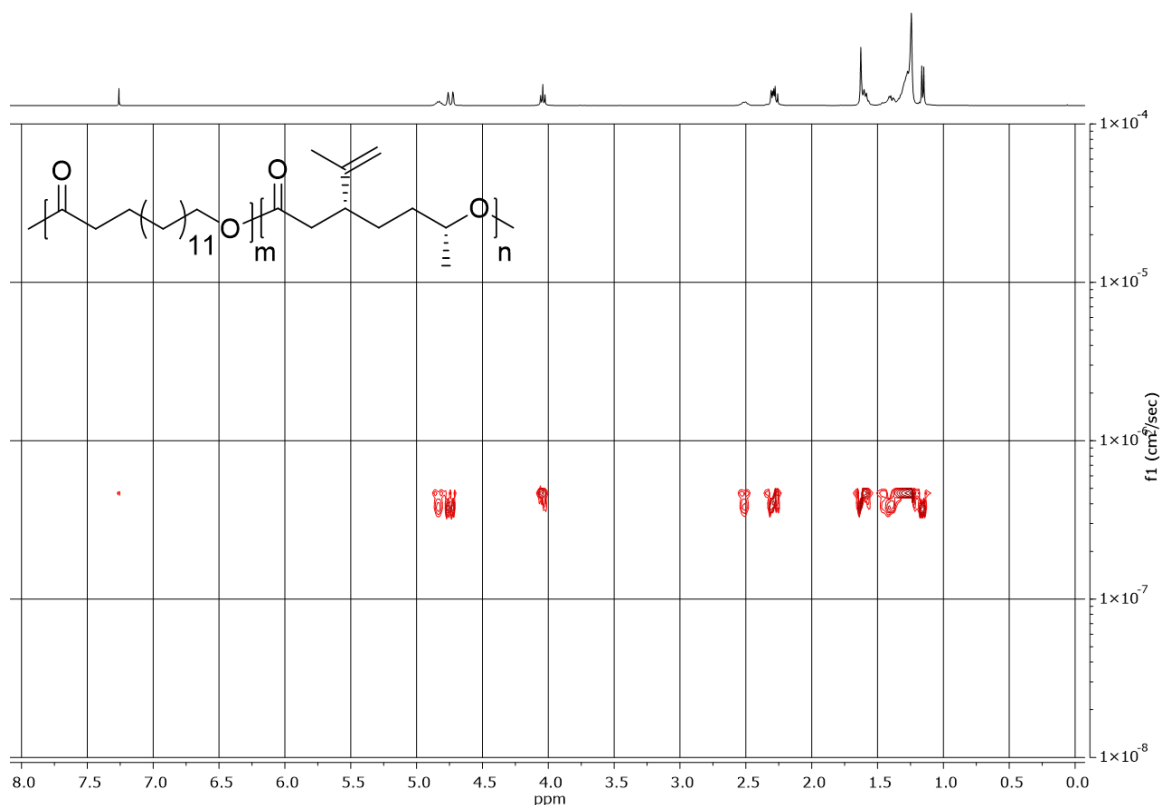


Figure S33: DOSY NMR spectrum of PPDL-*b*-PDHC (PPDL/PDHC=64/36; Table 2, Entry 1, CDCl_3 , 400 MHz, number of scans: 8, resolution factor: 1, repetitions: 1, points in diffusion dimension: 128).

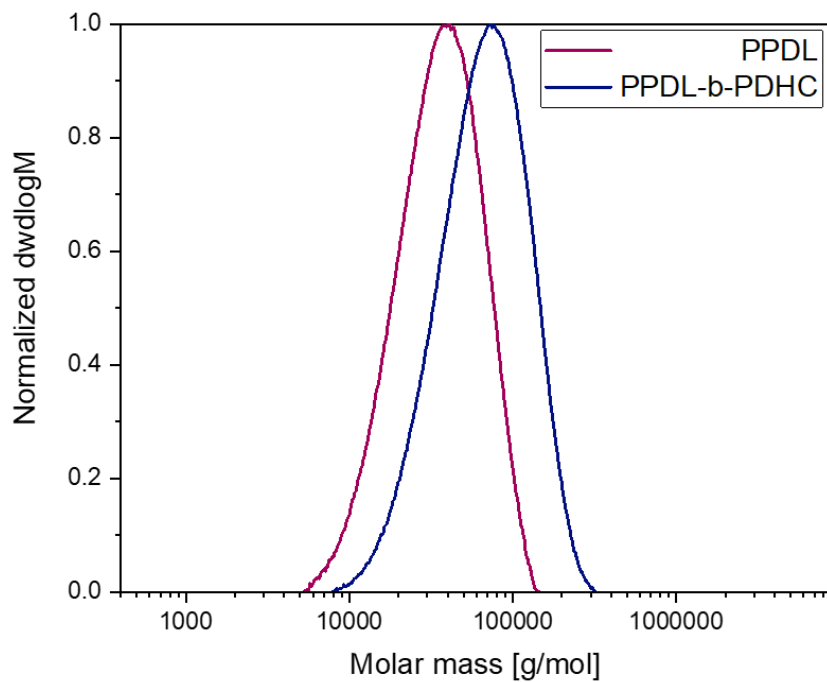


Figure S36: SEC traces of the first block (PPDL) and isolated polymer (PPDL-*b*-PDHC) (Table 2, Entry 1) synthesized with [(ONOO)^{*t*Bu}Y(bdsa)(THF)] catalyst.

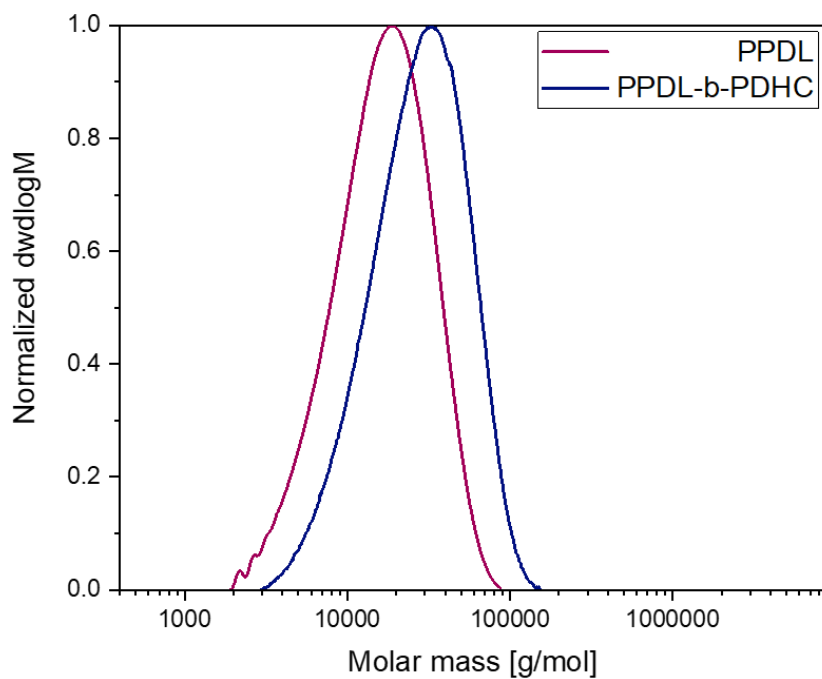


Figure S37: SEC traces of the first block (PPDL) and isolated polymer (PPDL-*b*-PDHC) (Table 2, Entry 3) synthesized with [(ONOO)^{*t*Bu}Y(*i*PrO)(THF)] catalyst.

Differential Scanning Calorimetry of PPDL-*b*-PDHC Copolymers

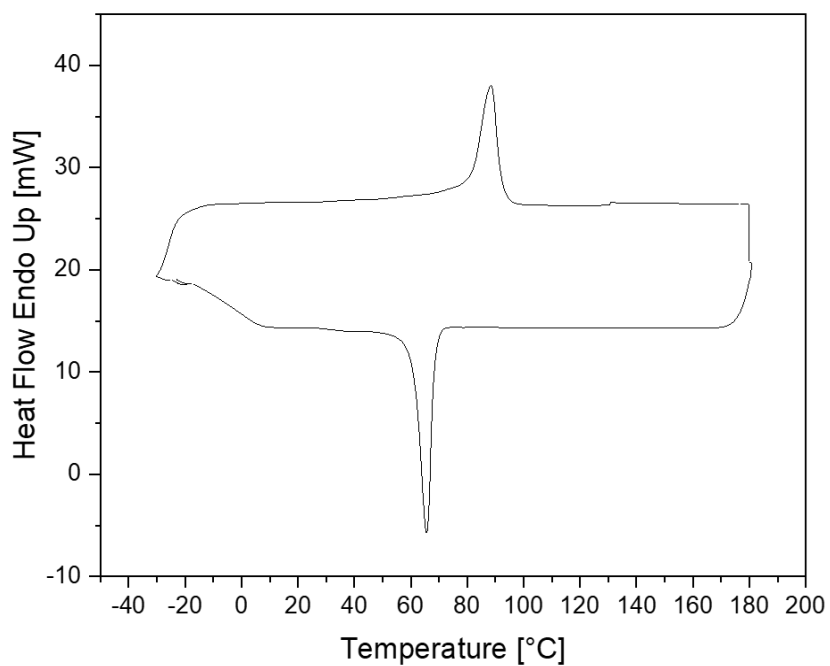


Figure S38: DSC analysis of PPDL-*b*-PDHC with $T_m = 88$ °C (Table 2, Entry 1).

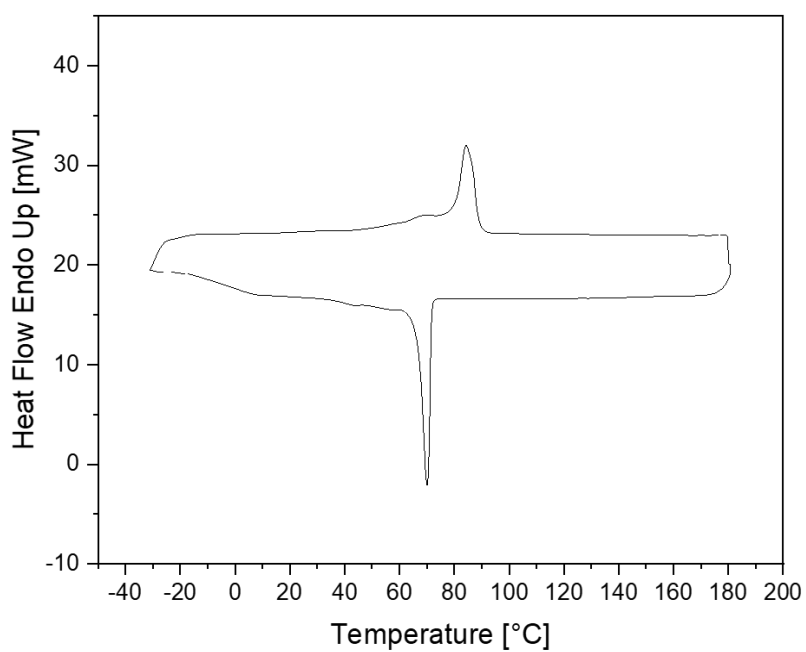


Figure S39: DSC analysis of PPDL-*b*-PDHC with $T_g = -18$ °C, and $T_m = 84$ °C (Table 2, Entry 2).

Powder X-ray Diffraction of Block Copolymers

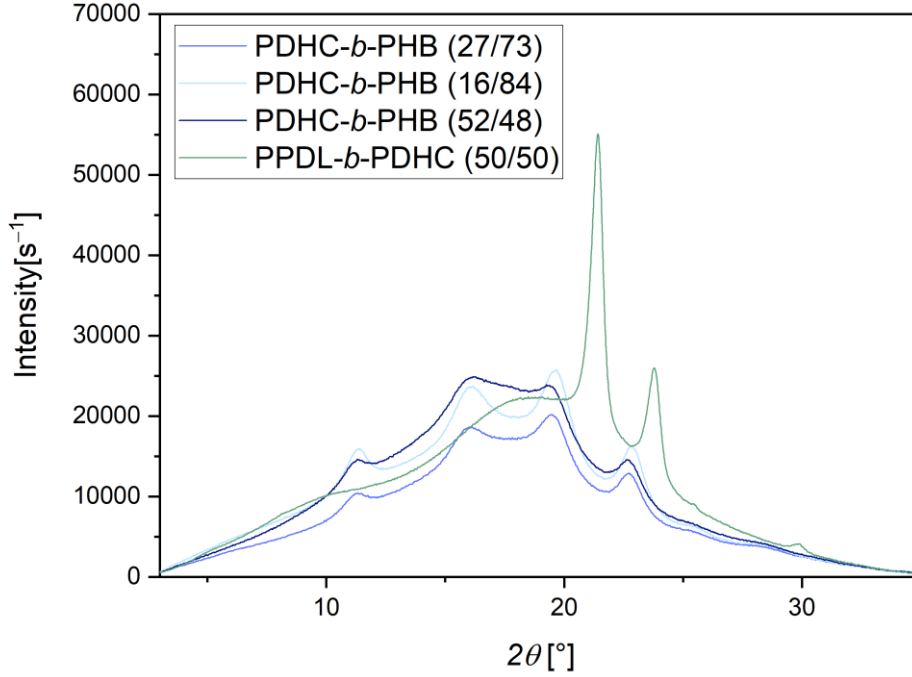


Figure S40: Baseline corrected data of PXRD measurements (PDHC-*b*-PHB (16/84): Table 2, Entry 5; PDHC-*b*-PHB (27/73): Table 2, Entry 7; PDHC-*b*-PHB (52/48): Table 2, Entry 6; PPDL-*b*-PDHC (50/50): Table 2, Entry 3).

Small-angle X-ray Scattering Analysis of PPDL-*b*-PDHC Copolymers

The analysis of the small-angle scattering data was performed with the open-source analysis software *SasView 6.0* by fitting the scattering curves with the following structural models.

1. Granular Structure

For all polymers, the small-angle scattering contribution, which results from the microscopic granular structure, was fitted using the model for a two-phase system developed by Porod⁷:

$$I_{\text{gran}}(q) = Sc \cdot \left(\frac{q}{q^*}\right)^{-\nu} \quad (\text{S1})$$

where Sc is the scaling factor, ν the Porod exponent and $q^* = 1 \text{ \AA}^{-1}$. For a two-phase system with a sharp interface, the Porod exponent $\nu = 4$ and the scaling factor $Sc = 2\pi (\rho_{\text{b,polymer}})^2 S/V (q^*)^{-4}$ can be expressed in terms of the overall scattering length density of the polymer $\rho_{\text{b,polymer}}$ and the surface-to-volume ratio S/V .

2. Structure of PPDL-containing polymers

The small-angle scattering curves of the PPDL-containing polymers were fitted by combining the contributions of the granular structure $I_{\text{gran}}(q)$ and incoherent scattering I_{inc} :

$$I_{\text{PPDL}}(q) = I_{\text{gran}}(q) + I_{\text{inc}}. \quad (\text{S2})$$

To relatively compare the size and order of the domains in these polymers, the scattering shoulder or peak in the residual scattering intensity $I(q) - I_{\text{gran}}(q)$, as shown in Figure S52, was fitted with the Gaussian peak shape function:

$$I_{\text{peak}}(q) = I_{\text{max}} \cdot \exp\left(-\frac{(q-q_{\text{max}})^2}{2\sigma^2}\right) + I_{\text{inc}}, \quad (\text{S3})$$

where I_{max} is the peak intensity, q_{max} the peak position and σ the standard deviation. The full width at half maximum (FWHM) of the scattering shoulder or peak is given by $\sim 2.355\sigma$. The fitting parameters according to Eq. S2 and S3 are both listed in Table S1.

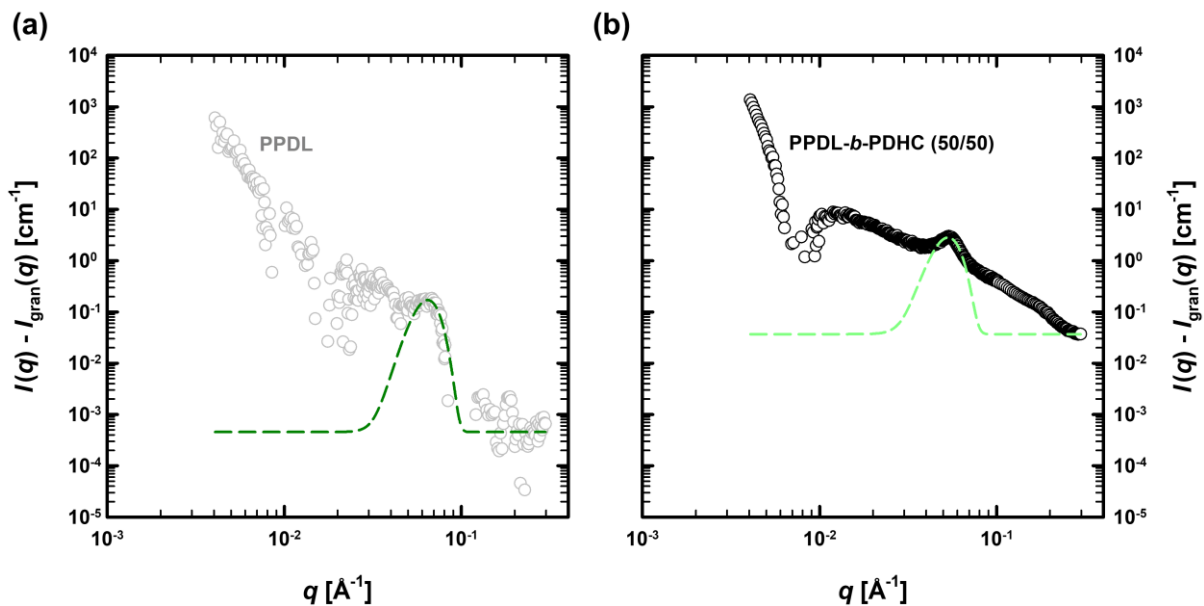


Figure S41: Residual scattering intensity $I(q) - I_{\text{gran}}(q)$ of (a) the PPDL homopolymer and (b) the block copolymer PPDL-*b*-PDHC with a block composition of 50/50 (Table 2, Entry 3). The shoulder or peak of the residual scattering curve was fitted with the Gaussian peak shape function from Eq. S3 (dashed green lines).

Table S1: Scaling factor S_c , Porod exponent ν and incoherent scattering contribution I_{inc} used to describe the scattering curves shown in Figure 3b according to Eq. S2 as well as peak intensity I_{max} , peak position q_{max} and standard deviation σ used to describe the residual scattering intensity shown in Figure S41 according to Eq. S3.

	PPDL	PPDL- <i>b</i> -PDHC (50/50)
$S_c / 10^{-6} \text{ cm}^{-1}$	5.36 ± 0.02	0.073 ± 0.002
ν	4.10 ± 0.01	4.23 ± 0.01
$I_{inc} / 10^{-2} \text{ cm}^{-1}$	0.045 ± 0.003	3.68 ± 0.08
I_{max} / cm^{-1}	0.171 ± 0.007	2.80 ± 0.01
$q_{max} / 10^{-2} \text{ \AA}^{-1}$	6.5 ± 0.3	5.32 ± 0.01
$\sigma / 10^{-3} \text{ \AA}^{-1}$	9 ± 2	8.1 ± 0.1

NMR Spectra of PDHC-*b*-PHB Copolymers

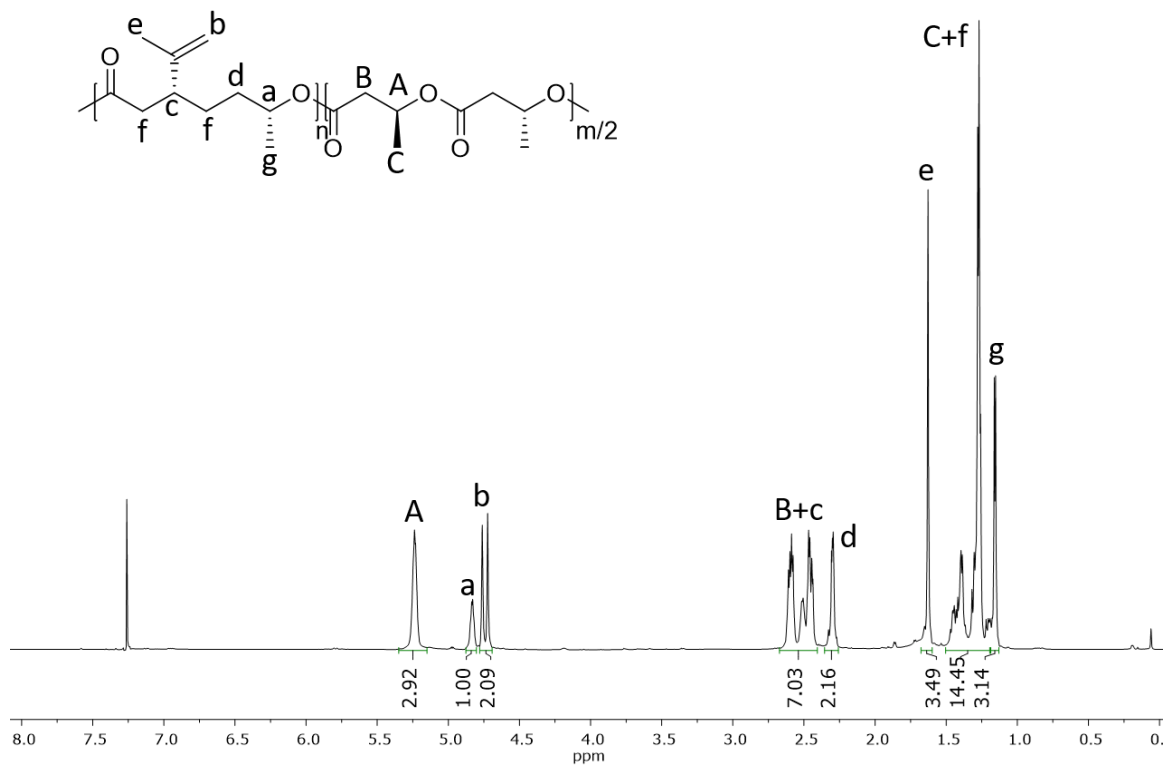


Figure S42: ¹H NMR spectrum of PDHC-*b*-PHB copolymer (PDHC/PHB = 27/73; Table 3, Entry 4, CDCl₃, 400 MHz).

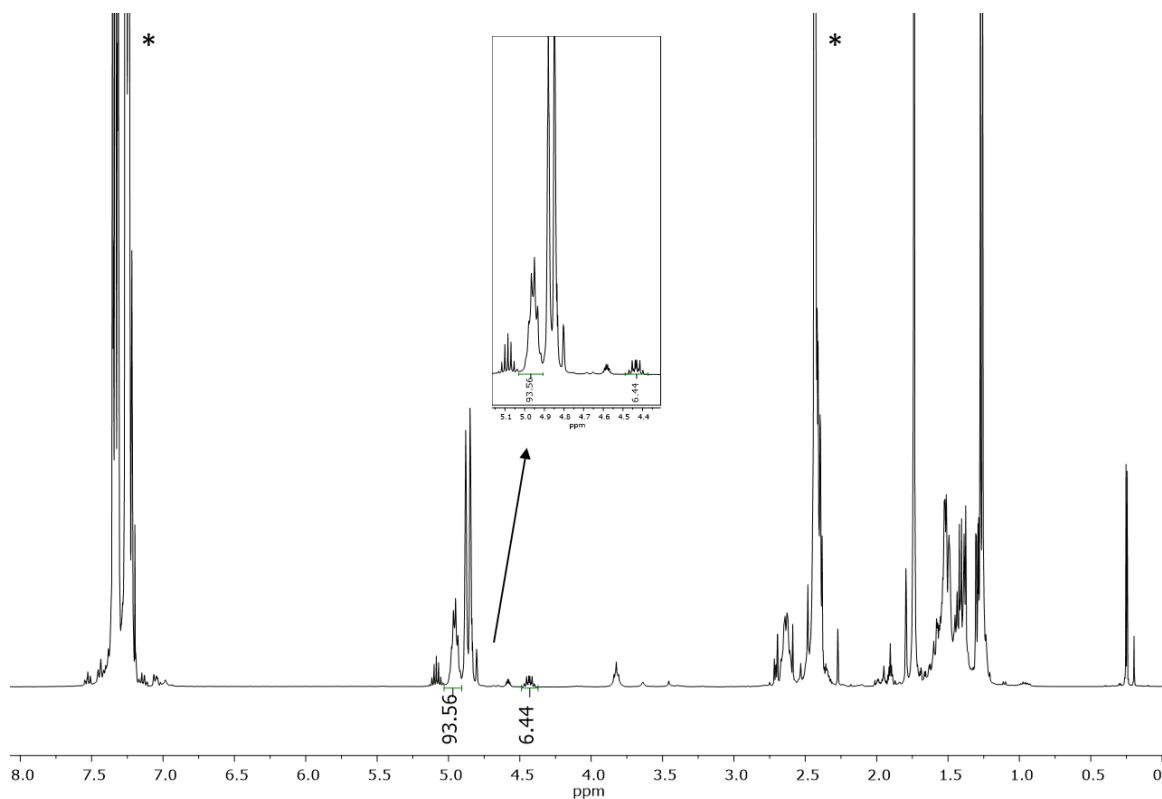


Figure S43: ^1H NMR spectrum of an aliquot of the with a DHC/PDHC mixture for conversion determination of DHC (Table 3, Entry 2, CDCl_3 , 400 MHz). (* = solvent)

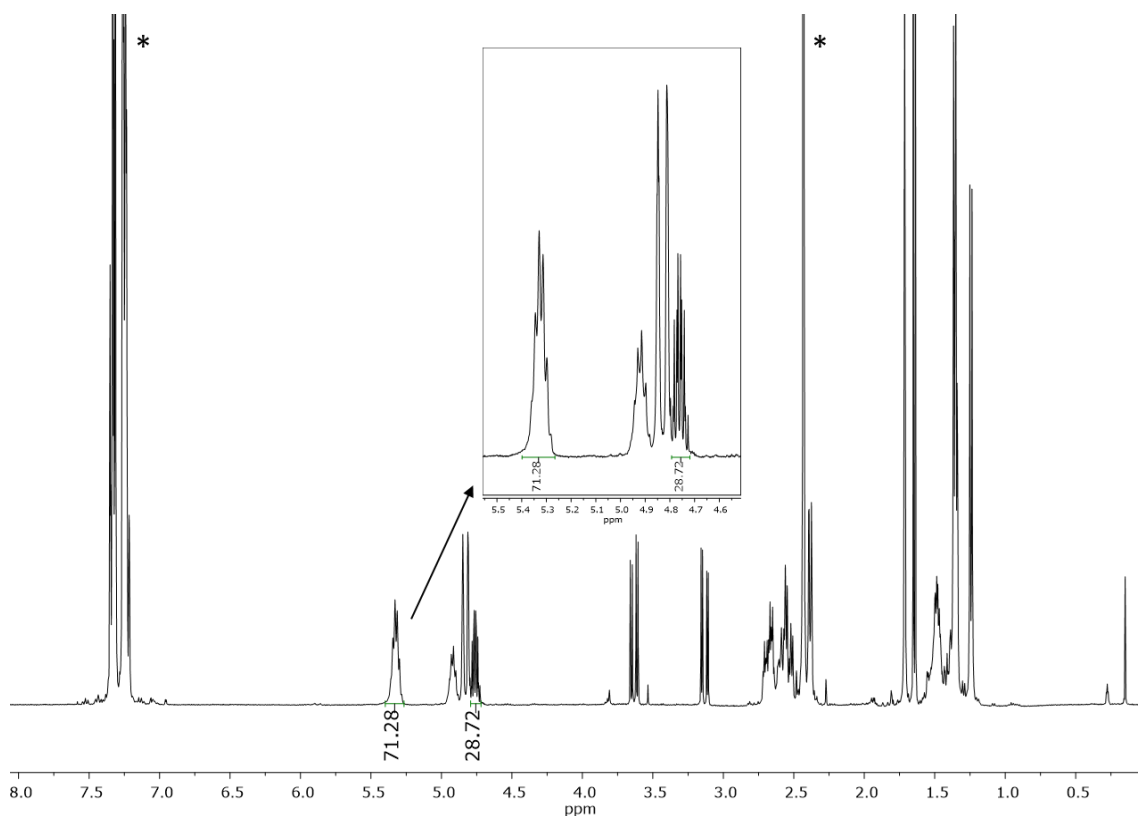


Figure S44: ^1H NMR spectrum of an aliquot of the second block with a DHC/PDHC and BBL/PHB mixture for conversion determination of BBL (Table 3, Entry 1, CDCl_3 , 400 MHz). (* = solvent)

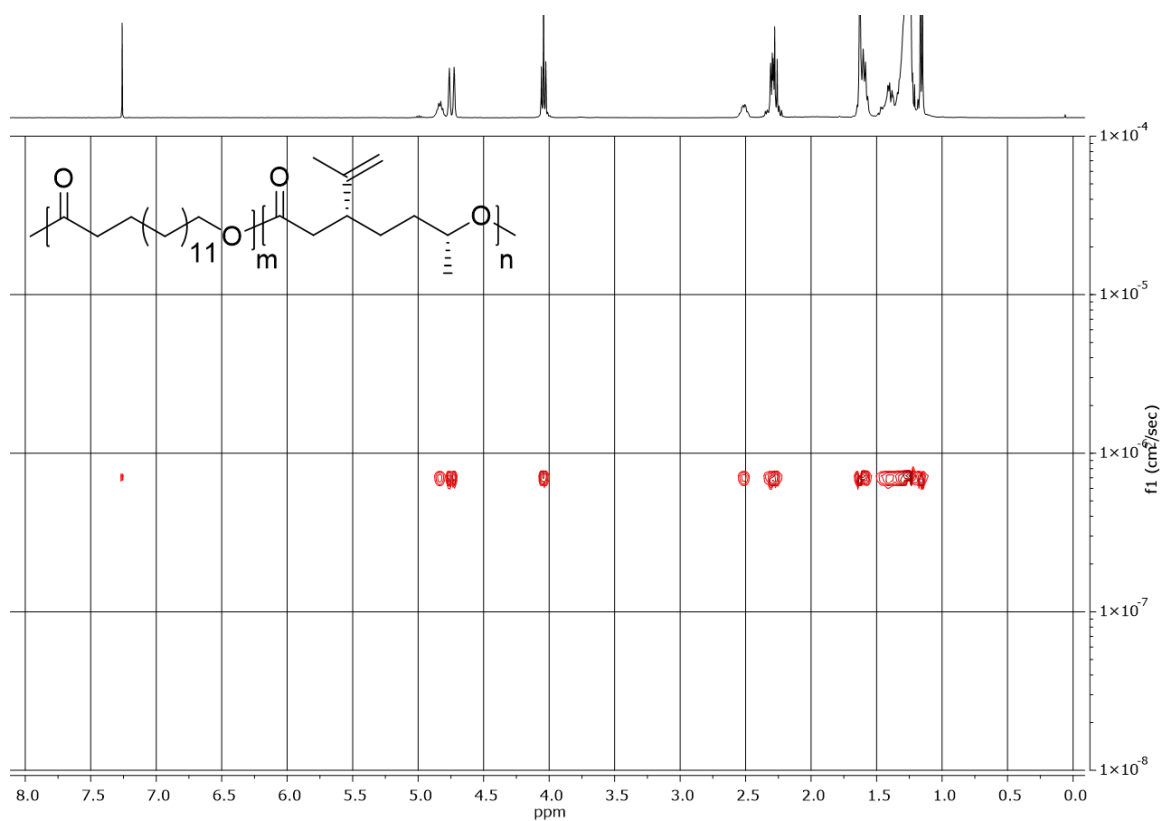


Figure S47: DOSY NMR spectrum of PDHC-*b*-PHB (PDHC/PHB=27/73; Table 3, Entry 4, CDCl₃, 700 MHz, number of scans: 8, resolution factor: 1, repetitions: 1, points in diffusion dimension: 128).

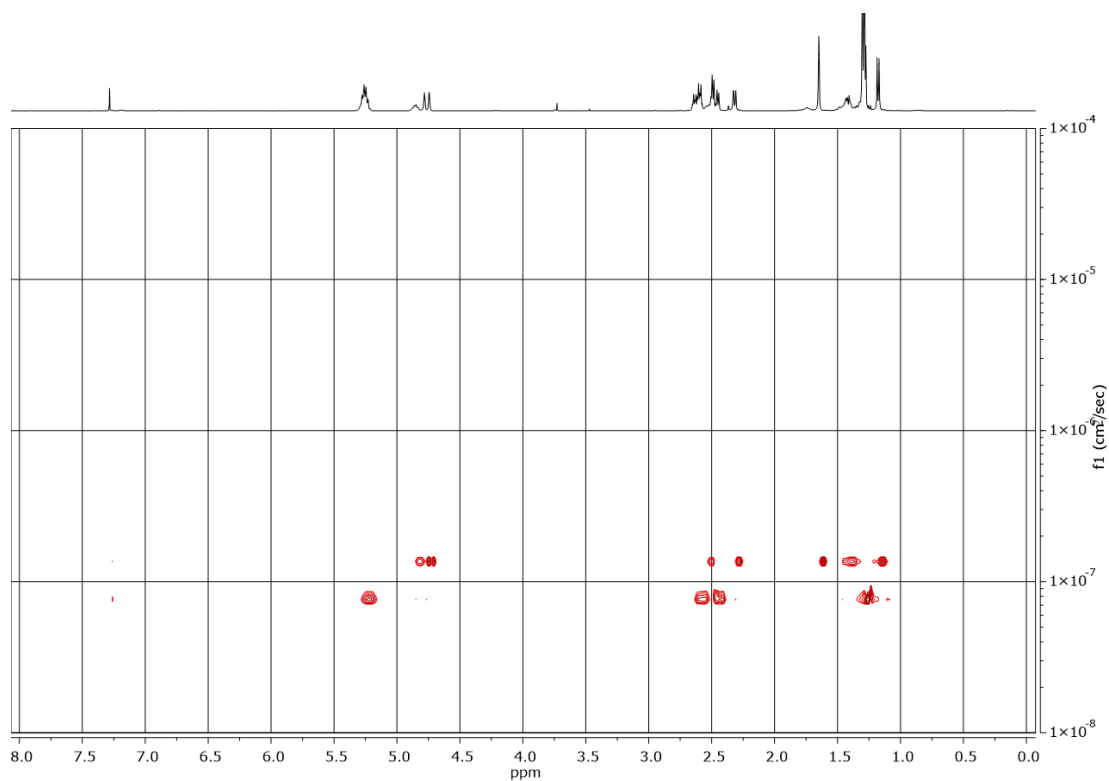


Figure S48: DOSY NMR spectrum of a blend from PDHC and PHB with the same composition as Table 3, Entry 4 (CDCl₃, 400 MHz, number of scans: 8, resolution factor: 1, repetitions: 1, points in diffusion dimension: 128).

SEC Traces of PDHC-*b*-PHB Copolymers

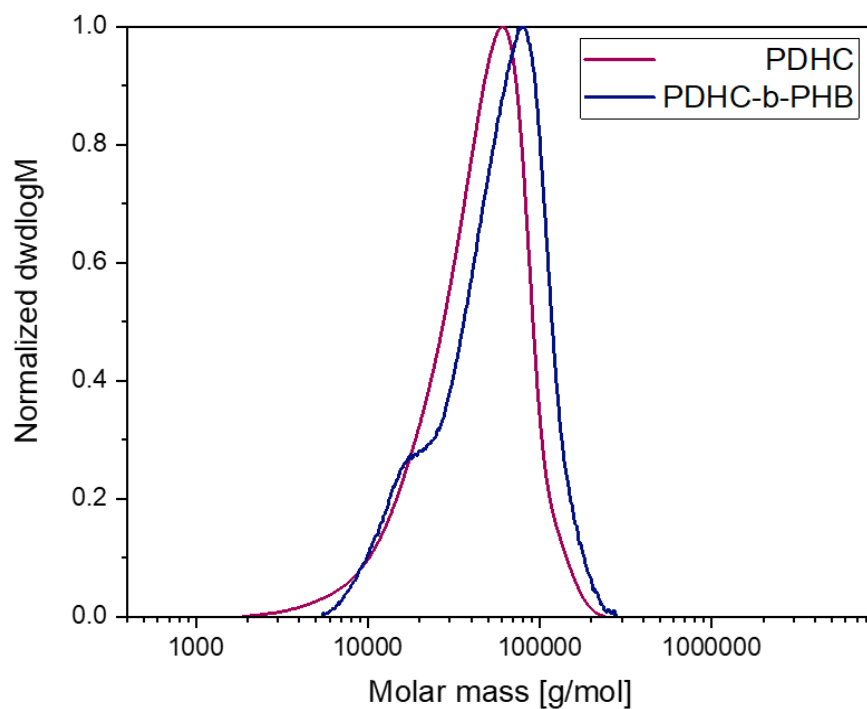


Figure S49: SEC traces of the first block (PDHC) and isolated polymer (PDHC-*b*-PHB) (Table 3, Entry 1) synthesized with [(ONOO)^{*t*}BuY(bdsa)(THF)] catalyst.

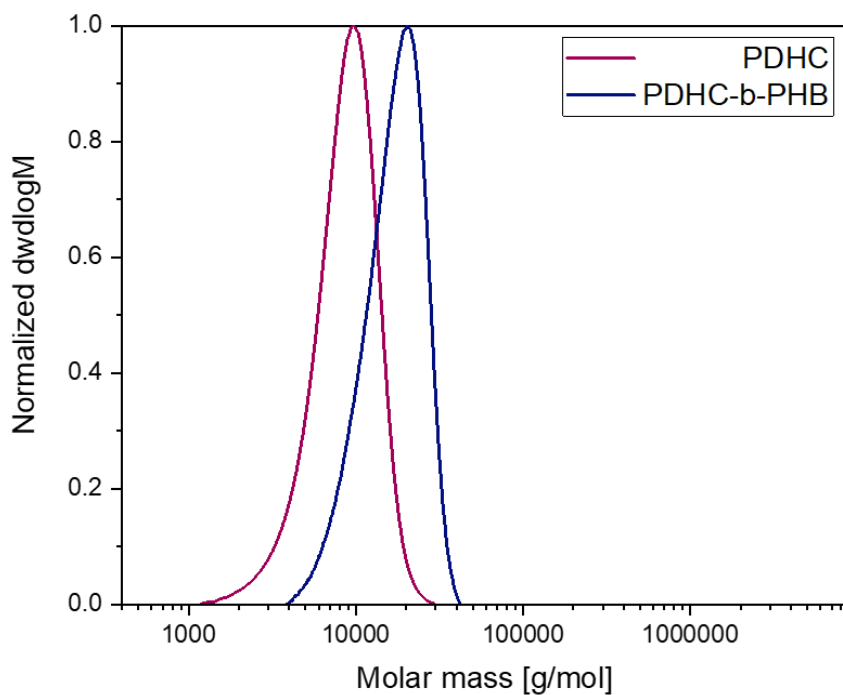


Figure S50: SEC traces of the first block (PDHC) and isolated polymer (PDHC-*b*-PHB) (Table 3, Entry 4) synthesized with [(ONOO)^{*t*}BuY(*i*PrO)(THF)] catalyst.

Differential Scanning Calorimetry of PDHC-*b*-PHB Copolymers

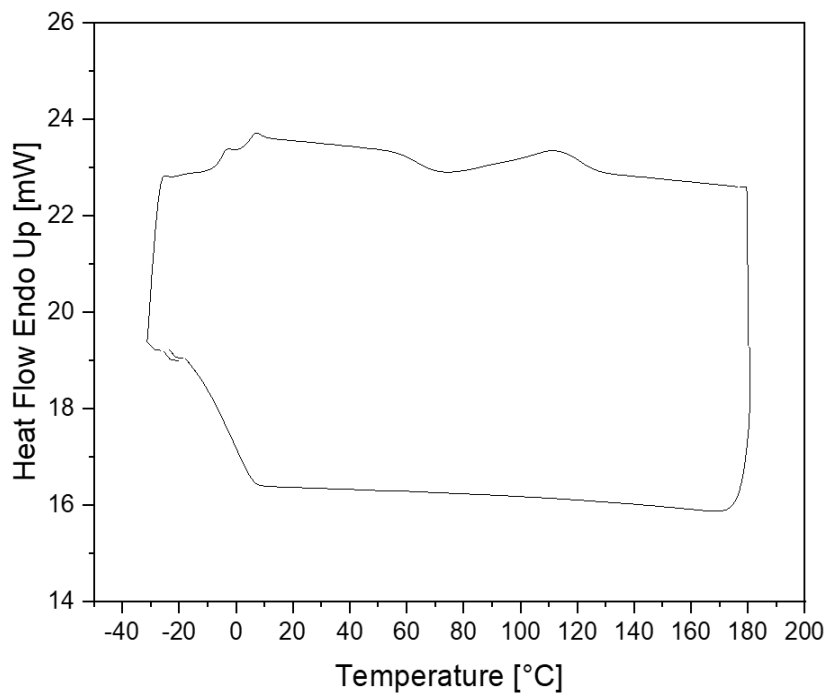


Figure S51: DSC analysis of PDHC-*b*-PHB with $T_{g,1} = -6$ °C, $T_{g,2} = -4$ °C, and $T_m = 112$ °C (Table 3, Entry 1).

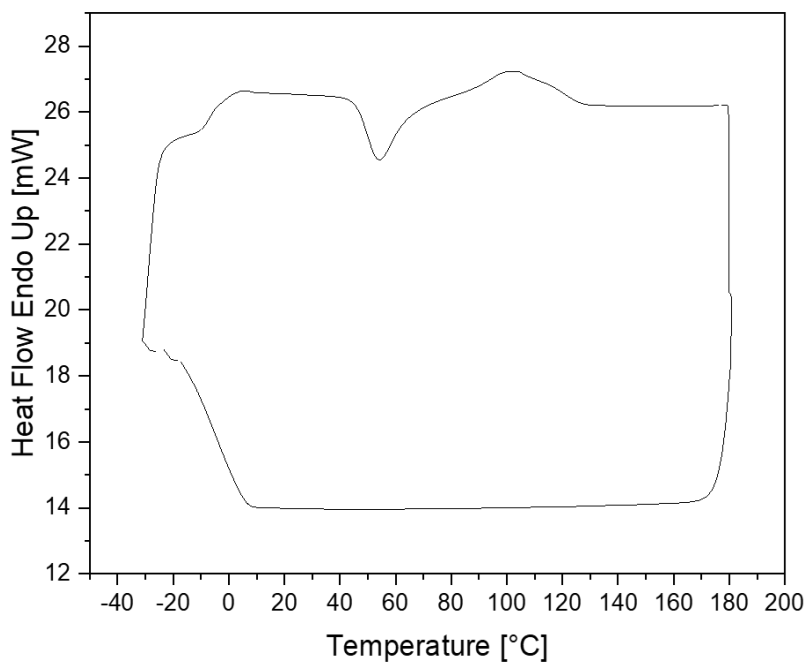


Figure S52: DSC analysis of PDHC-*b*-PHB produced with *i*PrOH with $T_{g,1} = -7$ °C, $T_{g,2} = 0$ °C, and $T_m = 103$ °C (Table 3, Entry 4).

Small-angle X-ray Scattering Analysis of PDHC-*b*-PHB Copolymers

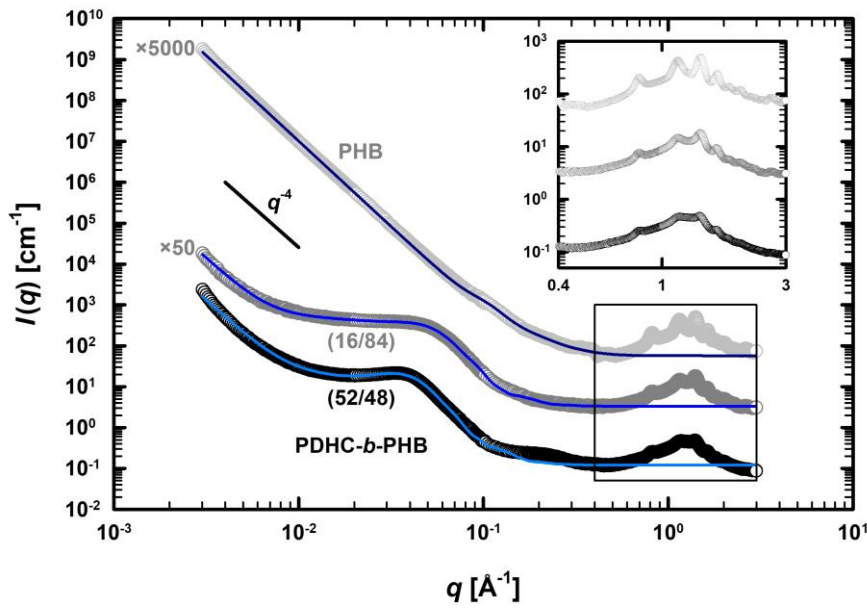


Figure S53: $I(q)$ -scattering curves of the PHB homopolymer (grey) and the PDHC-*b*-PHB block copolymers with block compositions of 16/84 (dark grey; Table 3, Entry 2) and 52/48 (black; Table 3, Entry 3). The scattering curves are fitted with Eq. S15 (blue lines). The fitting parameters are listed in Table S2. The scattering curves cover both small-angle and wide-angle scattering (inset), reproducing the results of the PXR measurements.

The small-angle scattering contribution from the amorphous domains of the semicrystalline PHB homopolymer as well as the semicrystalline PDHC-*b*-PHB block copolymers with block composition of 16/84 and 52/48 was fitted as follows:

$$I_{\text{dom}}(q) = n_{\text{dom}} \cdot P_{\text{sph}}(q) \cdot S_{\text{eff}}(q) \quad (\text{S4})$$

using the form factor of a randomly oriented spheroid $P_{\text{sph}}(q)$ and the effective structure factor $S_{\text{eff}}(q)$ as well as the number density of the amorphous domains in the polymer $n_{\text{dom}} = N/V_{\text{polymer}}$. The spheroid form factor is thereby given by⁸:

$$P_{\text{sph}}(q) = (\Delta\rho_{\text{b,dom}})^2 \cdot V_{\text{sph}}^2 \int_0^{\pi/2} F(q,\alpha)^2 \sin(\alpha) d\alpha, \quad (\text{S5})$$

with the scattering amplitude

$$F(q,\alpha) = \frac{3(\sin(qr) - qr \cos(qr))}{(qr)^3}, \quad (\text{S6})$$

where

$$r = \sqrt{R_e^2 \sin^2(\alpha) + R_p^2 \cos^2(\alpha)}, \quad (\text{S7})$$

$\Delta\rho_{\text{b,dom}}$ is the scattering length density contrast between the amorphous domains and crystalline portions of the polymer, $V_{\text{sph}} = 4/3 \pi R_e^2 R_p$ the volume of a single spheroid, R_p the polar radius along and R_e the equatorial radius perpendicular to the rotational axis of the spheroid.

Due to the anisotropic structure of the spheroids, the effective structure factor $S_{\text{eff}}(q)$ was calculated from the hard-sphere structure factor $S_{\text{HS}}(q)$ using the decoupling approximation developed by Kotlarchyk and Chen⁹:

$$S_{\text{eff}}(q) = 1 + \beta(q)(S_{\text{HS}}(q) - 1), \quad (\text{S8})$$

where

$$\beta(q) = \frac{\left(\int_0^{\pi/2} F(q,\alpha) \sin(\alpha) d\alpha\right)^2}{\int_0^{\pi/2} F(q,\alpha)^2 \sin(\alpha) d\alpha}. \quad (\text{S9})$$

The hard-sphere structure factor $S_{\text{HS}}(q)$ is defined as¹⁰⁻¹²:

$$S_{\text{HS}}(q) = \frac{1}{1 - 24\eta_{\text{eff}} G(2R_{\text{HS}}q)/(2R_{\text{HS}}q)}, \quad (\text{S10})$$

with

$$G(x) = \frac{a}{x^2} (\sin x - x \cos x) + \frac{b}{x^3} (2x \sin x + (2 - x^2) \cos x - 2) + \frac{c}{x^5} (-x^4 \cos x + 4(3x^2 - 6 \cos x + (x^3 - 6x) \sin x + 6)). \quad (\text{S11})$$

Here, R_{HS} is the hard-sphere radius and η_{eff} the effective hard-sphere volume fraction. The three parameters a , b and c are defined as follows in terms of η_{eff} :

$$a = \frac{(1+2\eta_{\text{eff}})^2}{(1-\eta_{\text{eff}})^4}, \quad (\text{S12})$$

$$b = \frac{-6\eta_{\text{eff}}(1+\eta_{\text{eff}}/2)^2}{(1-\eta_{\text{eff}})^4}, \quad (\text{S13})$$

$$c = \frac{\sigma}{2} \eta_{\text{eff}}. \quad (\text{S14})$$

The small-angle scattering curves of the PHB-containing polymer were then fitted by combining Eq. S1 and S4:

$$I_{\text{PHB}}(q) = I_{\text{gran}}(q) + \phi_p \cdot I_{\text{dom}}(q) + I_{\text{inc}}, \quad (\text{S15})$$

with the packing density $\phi_p = V_{\text{polymer}}/V_{\text{total}}$ of the polymer in the sample and the incoherent scattering contribution I_{inc} . The fitting parameters are listed in Table S2.

Table S2: Scaling factor Sc , Porod exponent ν , prefactor $\phi_s n_{\text{dom}} (\Delta\rho_{\text{b,dom}})^2$, polar radius R_p , equatorial radius R_e , hard-sphere radius R_{HS} , effective hard-sphere volume fraction η_{eff} and incoherent scattering contribution I_{inc} used to describe the scattering curves shown in Figure 4b and S53.

	PHB	PDHC- <i>b</i> -PHB (16/84)	PDHC- <i>b</i> -PHB (52/48)
$Sc / 10^{-6} \text{ cm}^{-1}$	8.88 ± 0.01	0.013 ± 0.003	0.066 ± 0.005
ν	4.18 ± 0.01	4.13 ± 0.04	4.12 ± 0.02
$\phi_s n_{\text{dom}} (\Delta\rho_{\text{b,dom}})^2 / 10^{-12} \text{ \AA}^{-4}$	0.87 ± 0.02	2.83 ± 0.01	3.68 ± 0.01
$R_p / \text{ \AA}$	4.96 ± 0.07	29.0 ± 0.1	38.8 ± 0.1
$R_e / \text{ \AA}$	27.5 ± 0.3	102 ± 1	136 ± 1
$R_{\text{HS}} / \text{ \AA}$	28.3 ± 0.2	45.3 ± 0.3	32.9 ± 0.3
η_{eff}	0.189 ± 0.004	0.295 ± 0.001	0.352 ± 0.001
$I_{\text{inc}} / 10^{-1} \text{ cm}^{-1}$	0.114 ± 0.001	0.658 ± 0.003	1.20 ± 0.01

2.4 Functionalization of Poly(dihydrocarvide) by a “Grafting from” Approach

NMR Spectroscopy of PDHC-2ME-OH

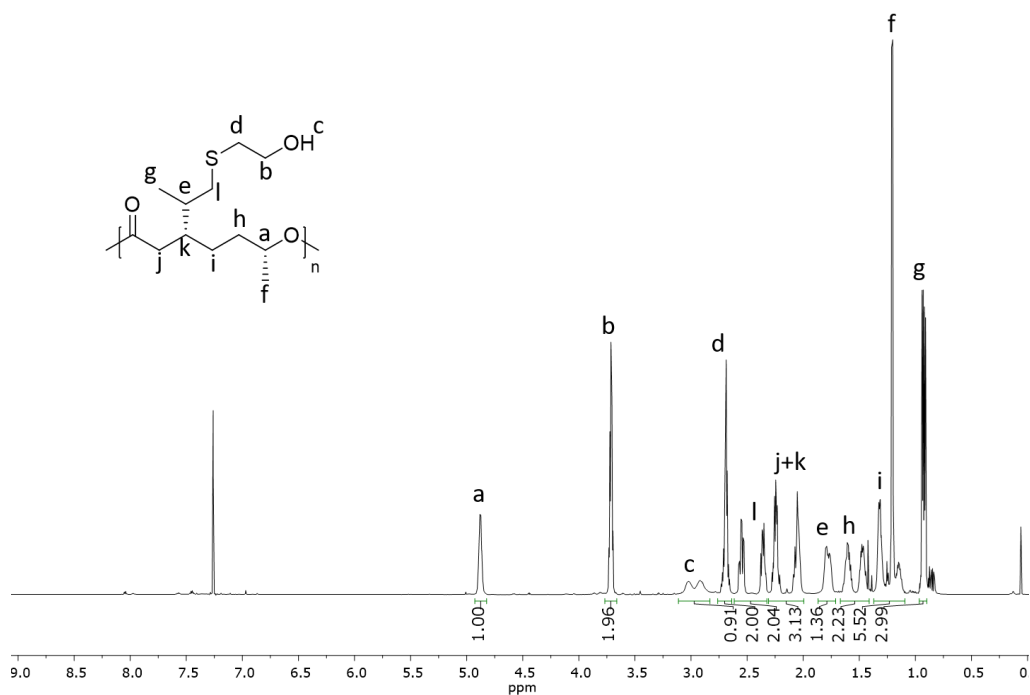


Figure S54: ¹H NMR spectrum of PDHC-2ME-OH (CDCl₃, 700 MHz).

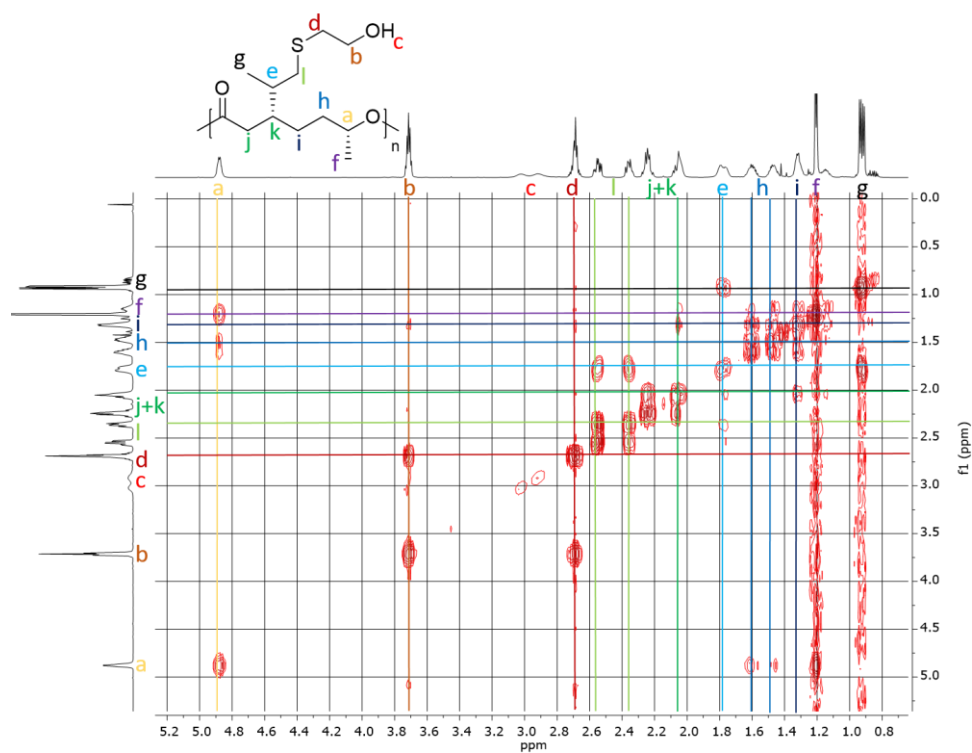


Figure S55: COSY NMR spectrum of PDHC-2ME-OH (CDCl₃, 700 MHz).

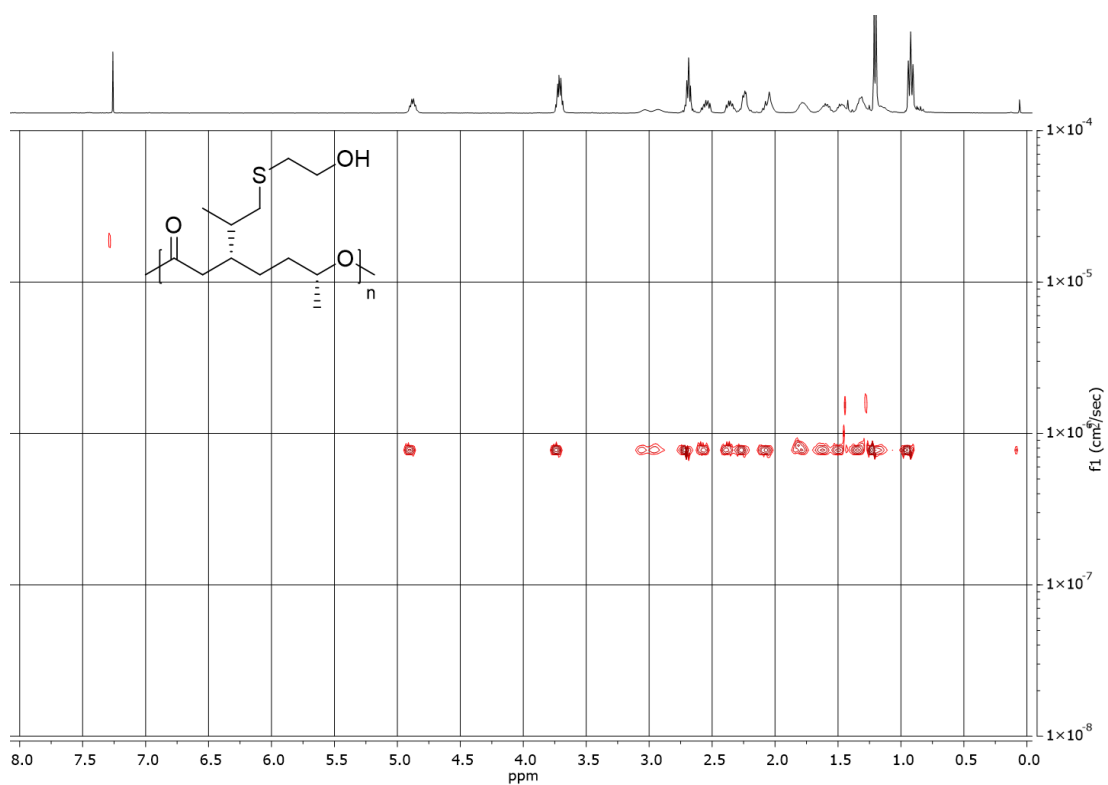


Figure S56: DOSY NMR spectrum of PDHC-2ME-OH (CDCl_3 , 400 MHz, number of scans: 8, resolution factor: 1, repetitions: 1, points in diffusion dimension: 128).

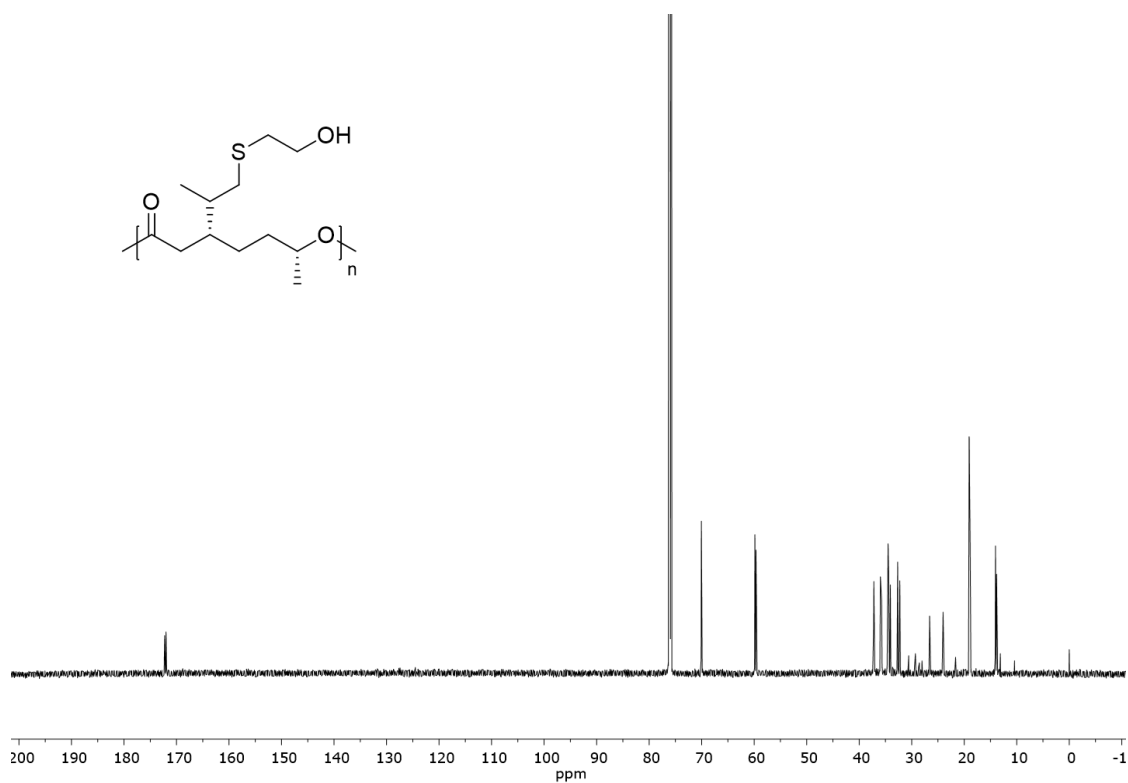


Figure S57: ^{13}C NMR spectrum of PDHC-2ME-OH (CDCl_3 , 176 MHz, 512 scans).

NMR Spectroscopy of PDHC-2ME-Br

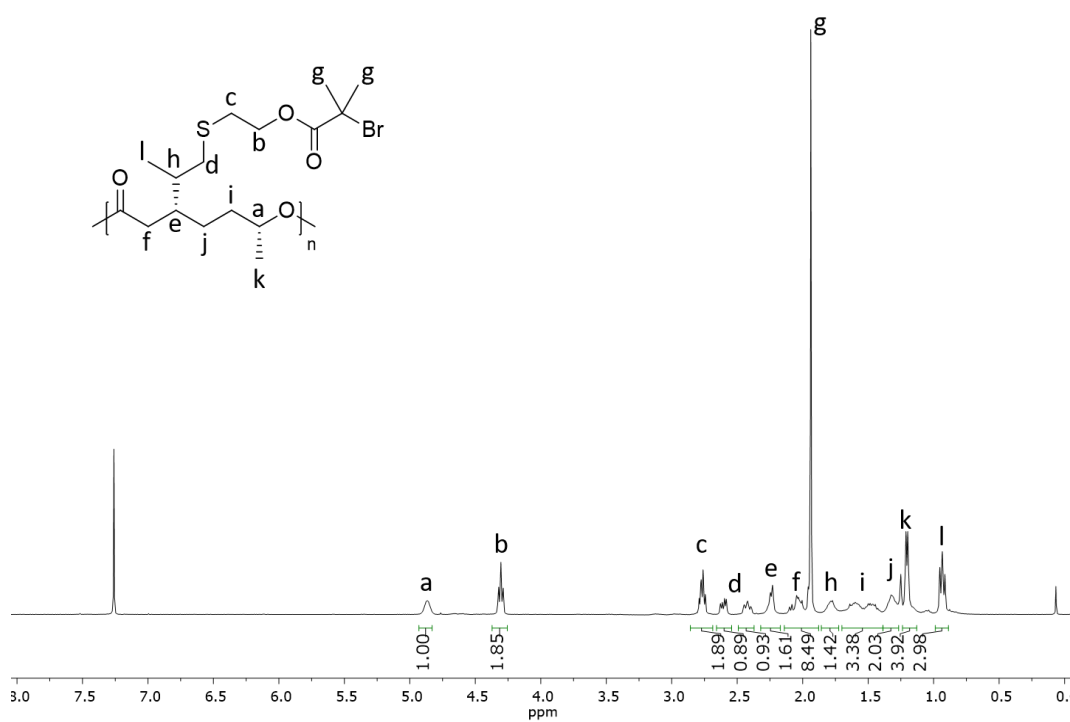


Figure S58: ¹H NMR spectrum of PDHC-2ME-Br (CDCl₃, 400 MHz).

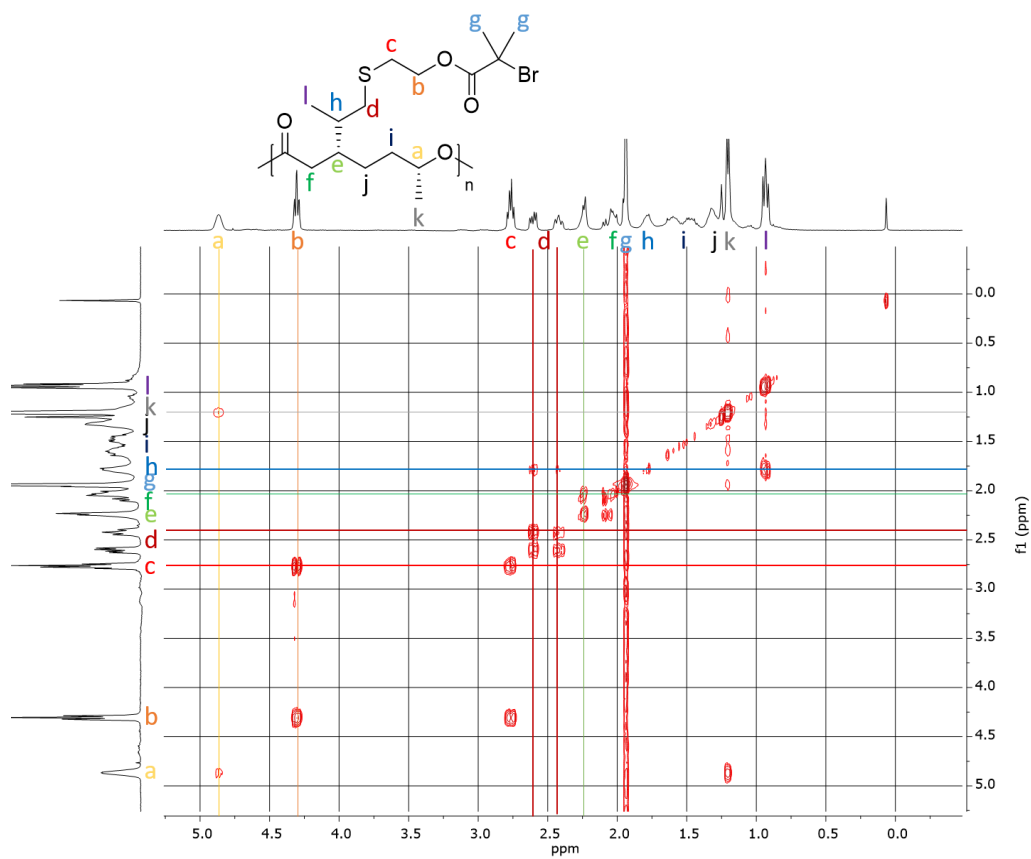


Figure S59: COSY NMR spectrum of PDHC-2ME-Br (CDCl₃, 400 MHz).

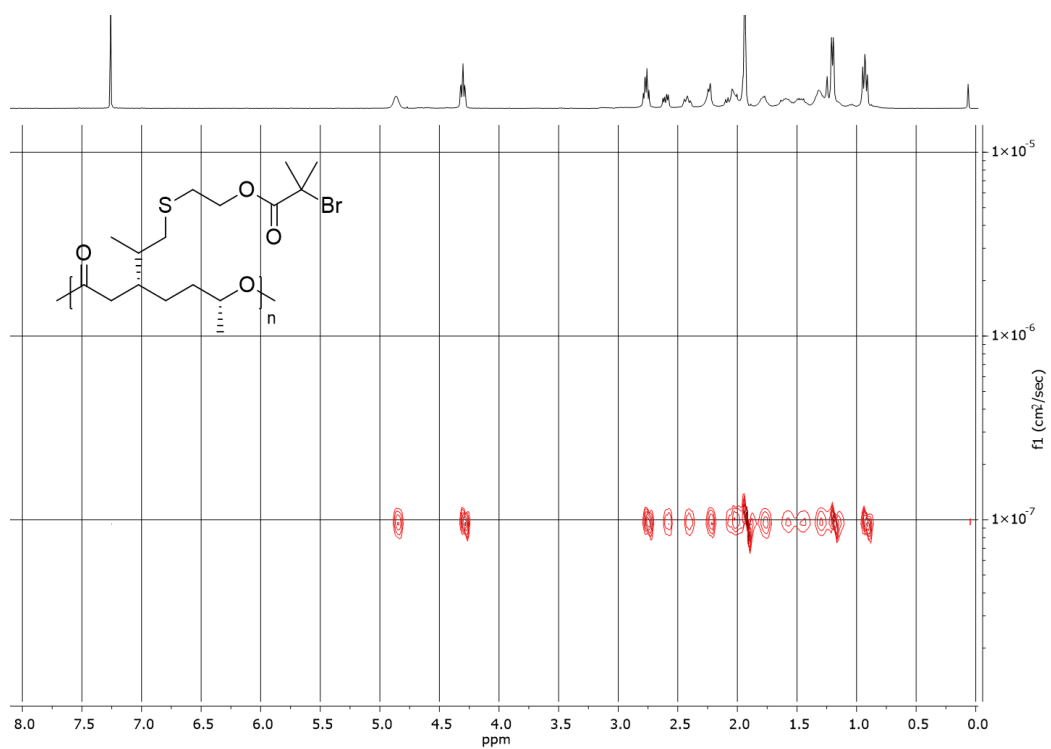


Figure S60: DOSY NMR spectrum of PDHC-2ME-Br (CDCl_3 , 400 MHz, number of scans: 8, resolution factor: 1, repetitions: 1, points in diffusion dimension: 128).

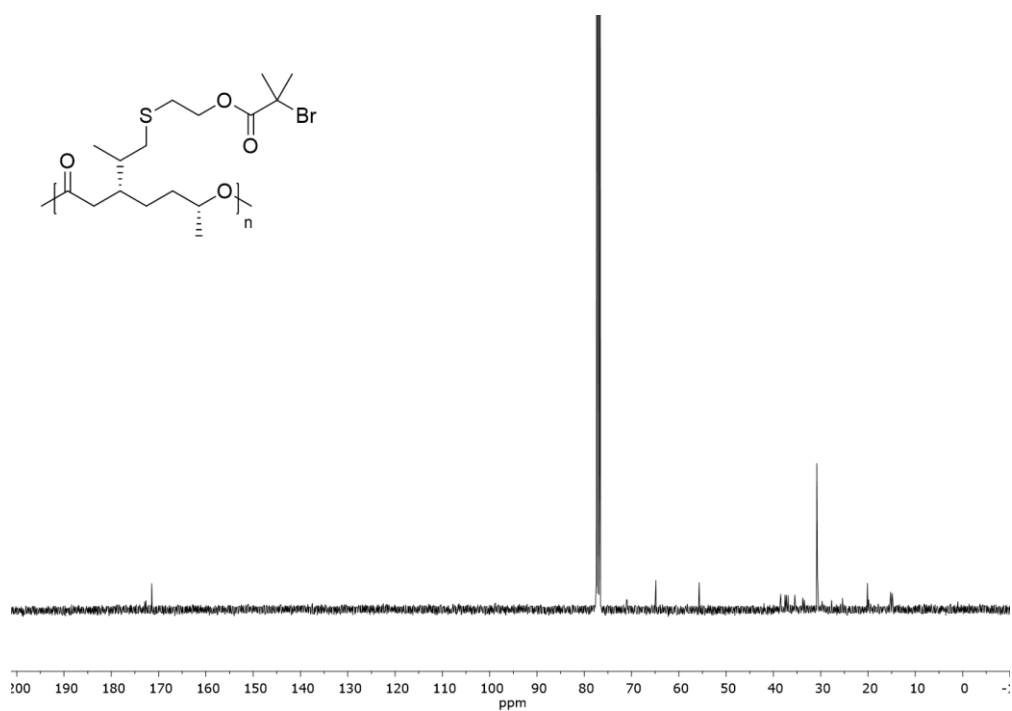


Figure S61: ^{13}C NMR spectrum of PDHC-2ME-Br (CDCl_3 , 101 MHz, 2048 scans).

SEC Traces

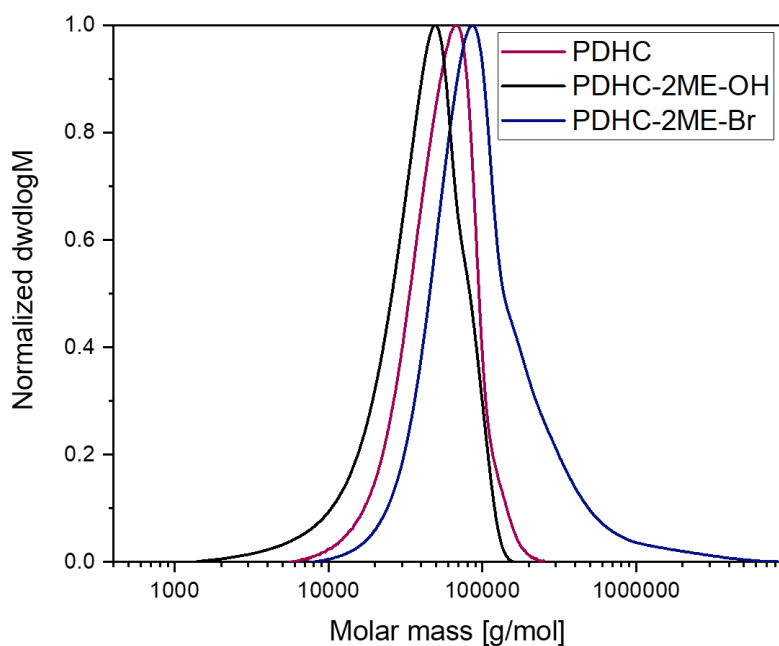


Figure S62: SEC traces of PDHC ($M_n = 45.3 \text{ kg mol}^{-1}$; $\mathcal{D} = 1.3$), PDHC-2ME-OH ($M_n = 28.8 \text{ kg mol}^{-1}$; $\mathcal{D} = 1.6$), and PDHC-2ME-Br ($M_n = 75.6 \text{ kg mol}^{-1}$; $\mathcal{D} = 2.3$).

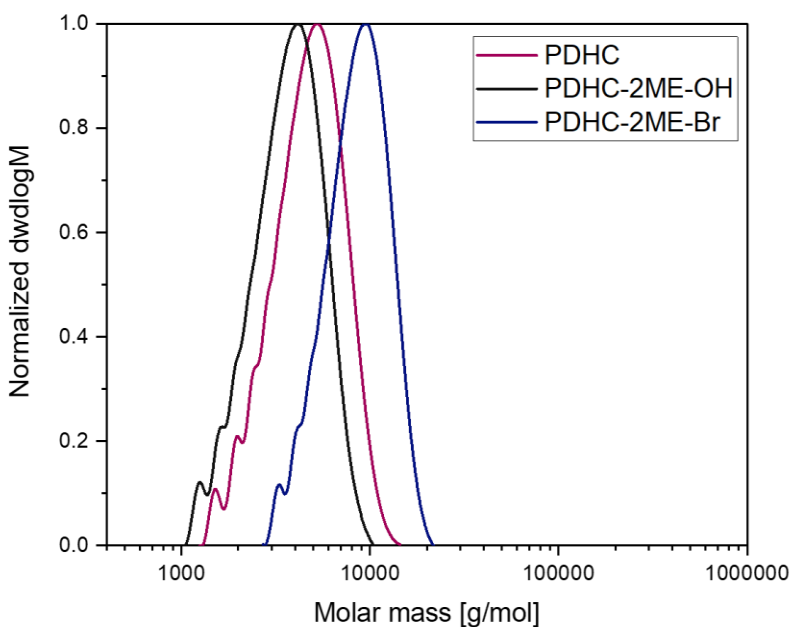


Figure S63: SEC traces of PDHC ($M_n = 4.2 \text{ kg mol}^{-1}$; $\mathcal{D} = 1.2$), PDHC-2ME-OH ($M_n = 3.3 \text{ kg mol}^{-1}$; $\mathcal{D} = 1.2$), and PDHC-2ME-Br ($M_n = 7.8 \text{ kg mol}^{-1}$; $\mathcal{D} = 1.2$).

Polymerization Studies

SARA ATRP

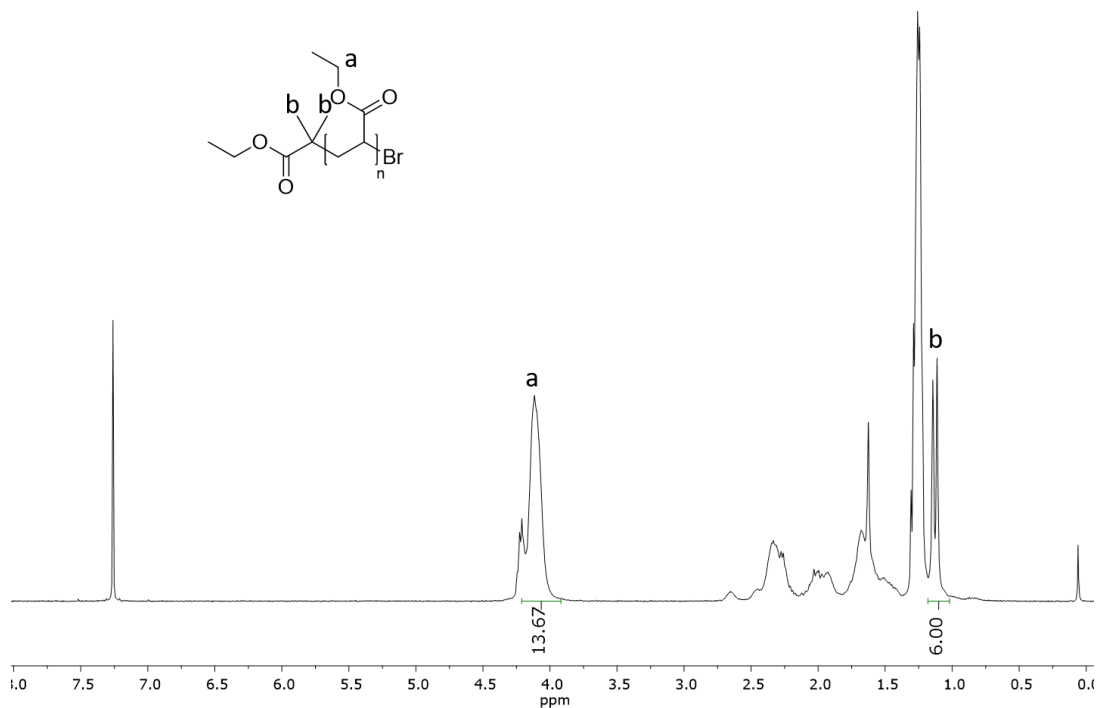


Figure S64: ¹H NMR spectrum of PEA synthesized via SARA ATRP with ethyl-2-bromoisobutyrate as initiator (DP = 7; CDCl₃, 400 MHz).

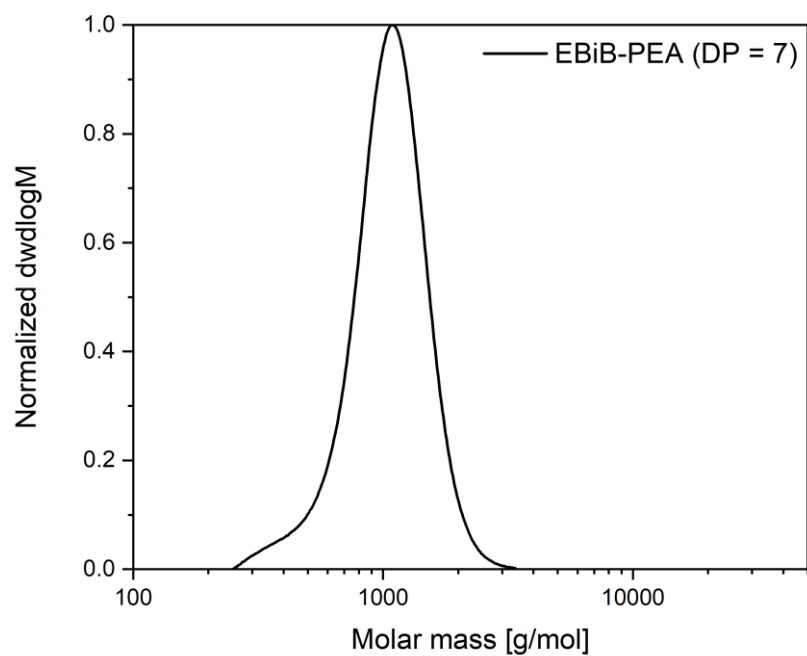


Figure S65: SEC traces of EBiB-PEA grafted via SARA ATRP with ethyl-2-bromoisobutyrate as initiator and ethyl acrylate (DP = 7; M_n = 0.97 kg mol⁻¹; Đ = 1.1) (black), measured in CHCl₃ relative to polystyrene.

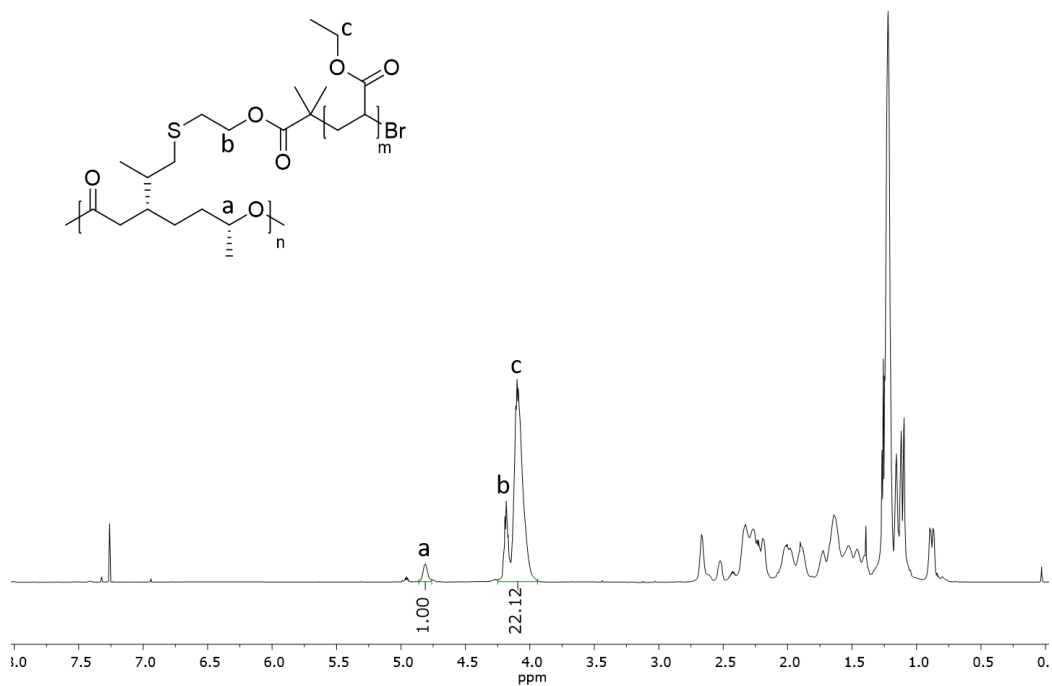


Figure S66: ^1H NMR spectrum of PDHC-g-PEA grafted via SARA ATRP with DP = 10 (CDCl_3 , 700 MHz).

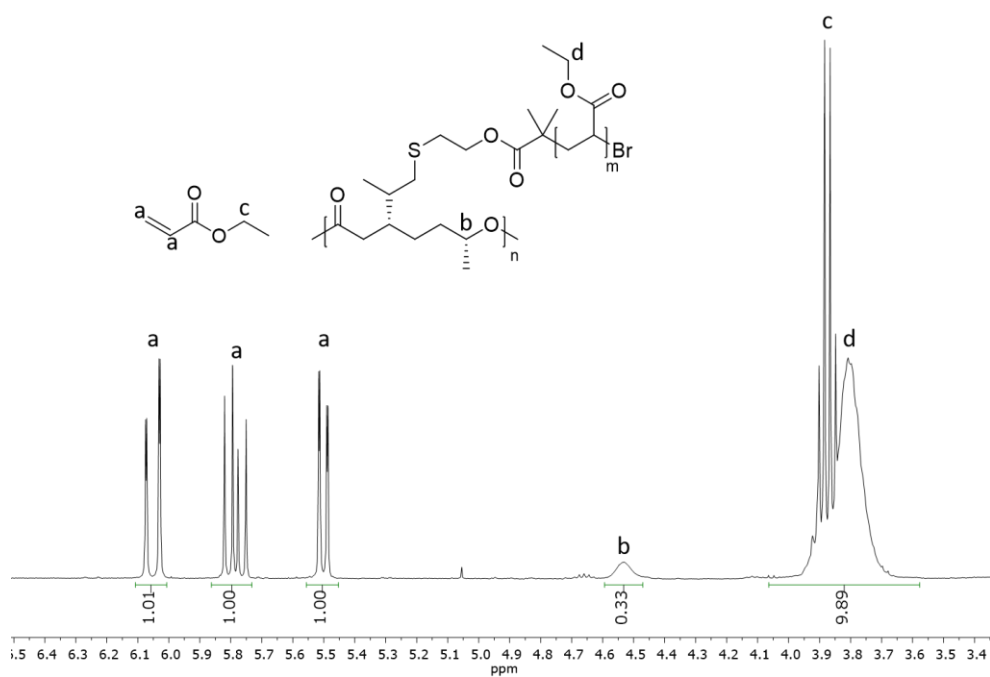


Figure S67: ^1H NMR spectrum of PDHC-g-PEA grafted via SARA ATRP with 10 equivalents of ethyl acrylate for the determination of the ethyl acrylate conversion (conversion = 80 %; CDCl_3 , 400 MHz).

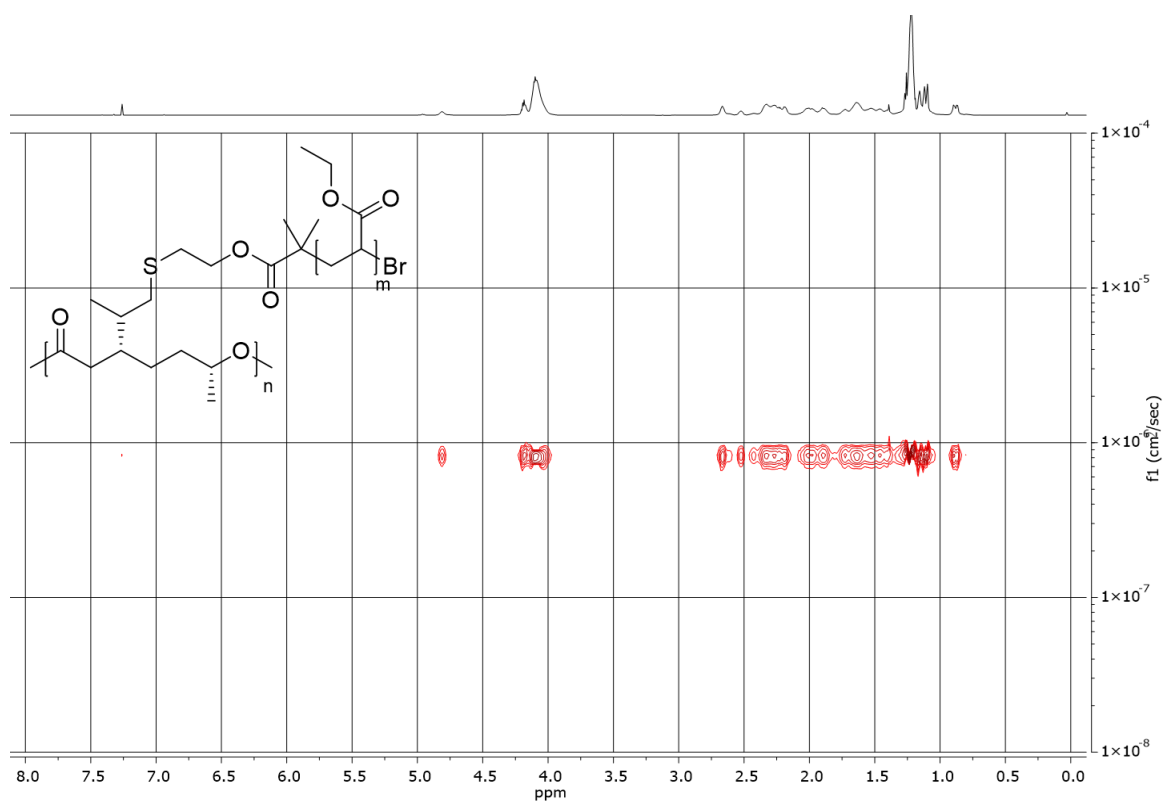


Figure S68: DOSY NMR spectrum of PDHC-*g*-PEA grafted via SARA ATRP with DP = 10 (CDCl₃, 400 MHz, number of scans: 16, resolution factor: 1, repetitions: 1, points in diffusion dimension: 128).

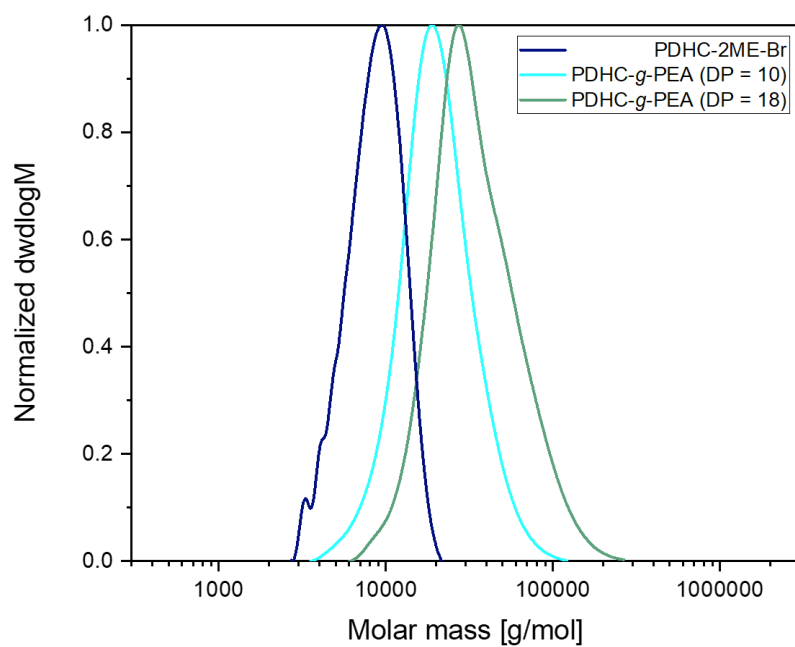


Figure S69: SEC traces of PDHC-2ME-Br ($M_n = 7.8 \text{ kg mol}^{-1}$; $\mathcal{D} = 1.2$), PDHC-*g*-PEA with DP = 10 ($M_n = 17.6 \text{ kg mol}^{-1}$; $\mathcal{D} = 1.3$), and PDHC-*g*-PEA with DP = 18 ($M_n = 28.7 \text{ kg mol}^{-1}$; $\mathcal{D} = 1.4$), synthesized via SARA ATRP.

ARGET ATRP

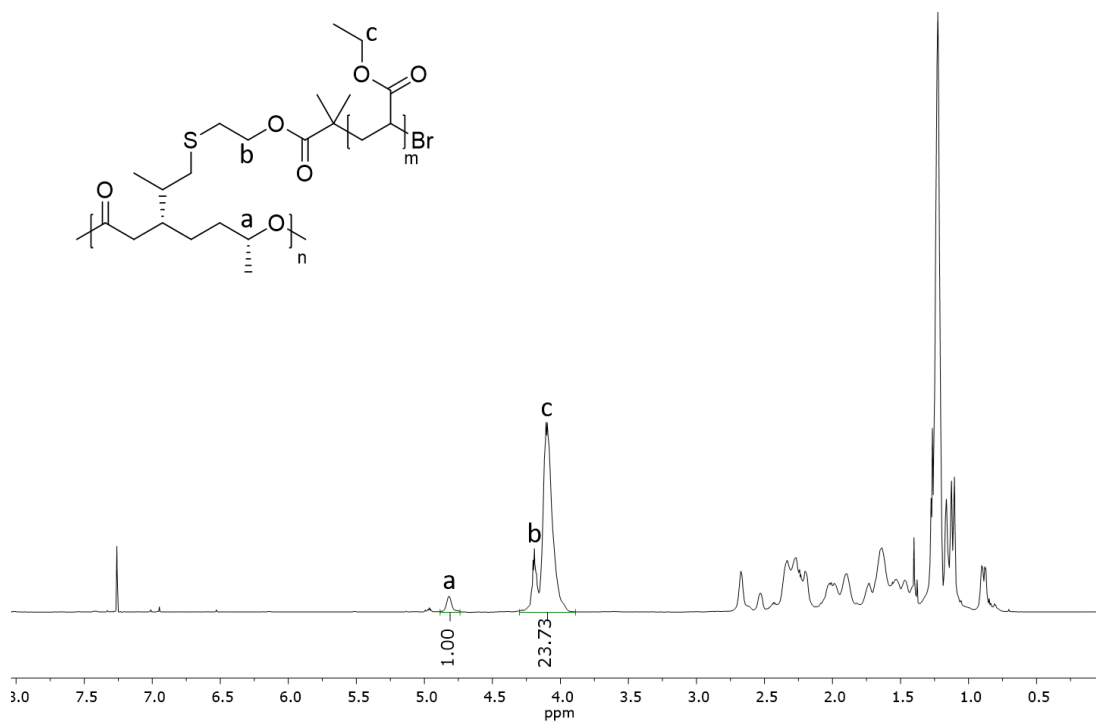


Figure S70: ^1H NMR spectrum of PDHC-g-PEA grafted via ARGET ATRP with DP = 11 (CDCl_3 , 700 MHz).

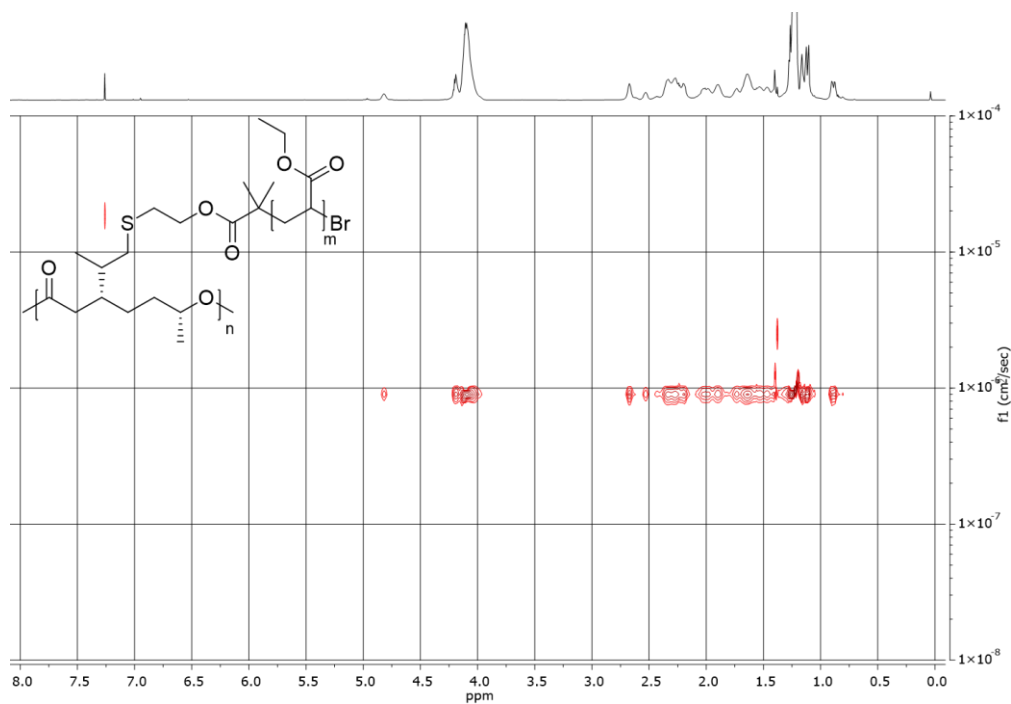


Figure S71: DOSY NMR spectrum of PDHC-g-PEA grafted via ARGET ATRP with DP = 11 (CDCl_3 , 700 MHz, number of scans: 24, resolution factor: 1, repetitions: 1, points in diffusion dimension: 128).

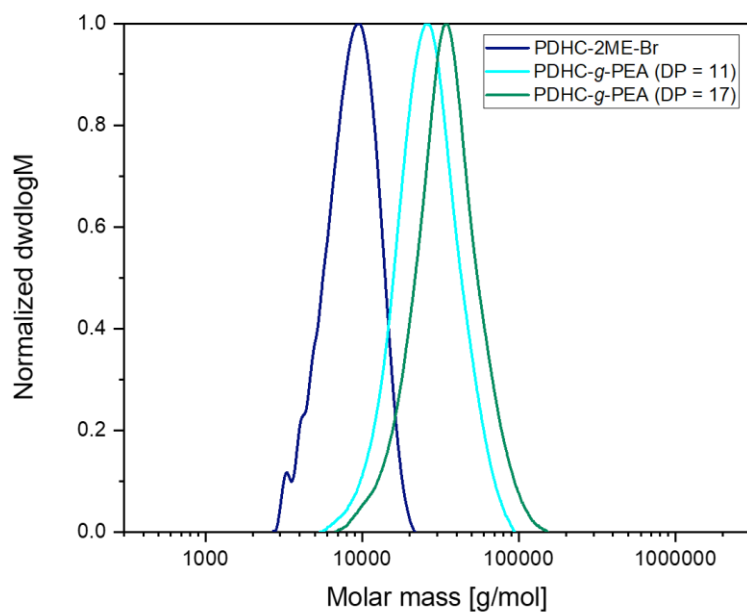


Figure S72: SEC traces of PDHC-2ME-Br ($M_n = 7.8 \text{ kg mol}^{-1}$; $\bar{D} = 1.2$), PDHC-*g*-PEA with DP = 11 ($M_n = 23.4 \text{ kg mol}^{-1}$; $\bar{D} = 1.2$), and PDHC-*g*-PEA with DP = 17 ($M_n = 30.5 \text{ kg mol}^{-1}$; $\bar{D} = 1.3$), synthesized via ARGET ATRP, measured in CHCl_3 relative to polystyrene standards.

Thermal Analysis

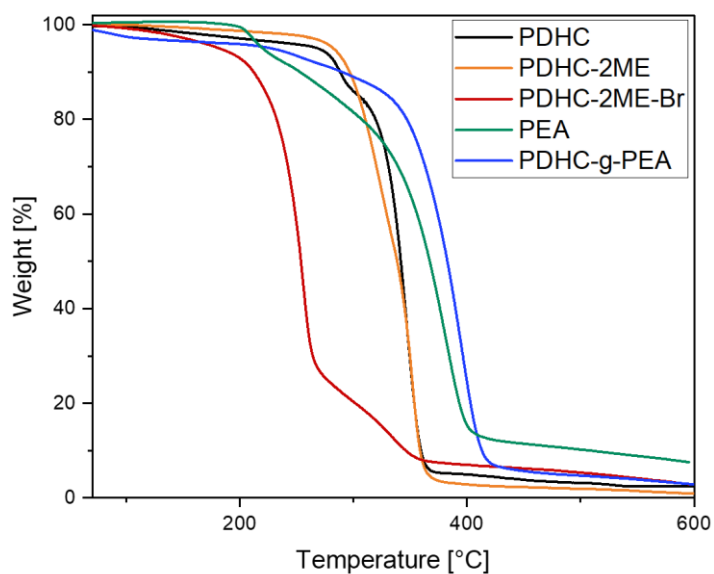


Figure S73: Thermogravimetric analysis of PDHC (Table 1, Entry 3), PDHC-2ME-OH, PDHC-2ME-Br, PEA with 10 equivalents of ethyl acrylate, PDHC-*g*-PEA synthesized via grafted from reaction via SARA ATRP with 10 equivalents of ethyl acrylate.

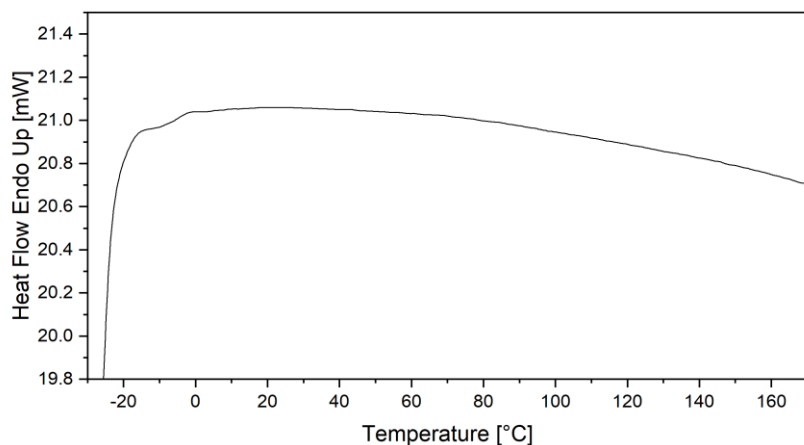


Figure S74: Section of the DSC analysis of PDHC-2ME-Br with $T_g = -5$ °C.

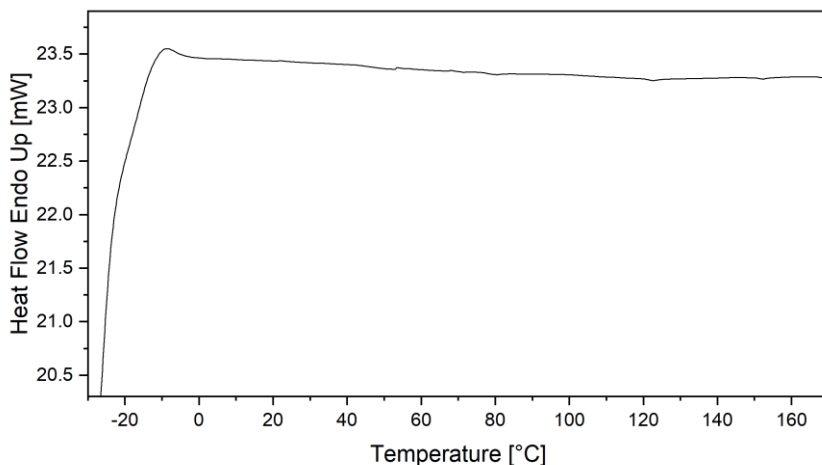


Figure S75: Section of the DSC analysis of PDHC-g-PEA synthesized via SARA ATRP grafted from approach with 15 equivalents of ethyl acrylate.

Literature

1. K. C. Hultsch, P. Voth, K. Beckerle, T. P. Spaniol and J. Okuda, *Organometallics*, 2000, **19**, 228-243.
2. E. Y. Tshuva, S. Groysman, I. Goldberg, M. Kol and Z. Goldschmidt, *Organometallics*, 2002, **21**, 662-670.
3. C.-X. Cai, L. Toupet, C. W. Lehmann and J.-F. Carpentier, *J. Organomet. Chem.*, 2003, **683**, 131-136.
4. L. Jia, D. Cui, J. Bignon, A. Di Cicco, J. Wdzieczak-Bakala, J. Liu and M.-H. Li, *Biomacromolecules*, 2014, **15**, 2206-2217.
5. T. G. Ribelli, M. Fantin, J.-C. Daran, K. F. Augustine, R. Poli and K. Matyjaszewski, *J. Am. Chem. Soc.*, 2018, **140**, 1525-1534.
6. J. R. Lowe, M. T. Martello, W. B. Tolman and M. A. Hillmyer, *Polym. Chem.*, 2011, **2**, 702-708.
7. G. Porod, *Kolloid-Zeitschrift*, 1951, **124**, 83-114.
8. A. Guinier, *Ann. Phys.*, 1939, **11**, 161-237.
9. M. Kotlarchyk and S. H. Chen, *J. Chem. Phys.*, 1983, **79**, 2461-2469.
10. J. K. Percus and G. J. Yevick, *Phys. Rev.*, 1958, **110**, 1.
11. M. Wertheim, *Phys. Rev. Lett.*, 1963, **10**, 321.
12. D. J. Kinning and E. L. Thomas, *Macromolecules*, 1984, **17**, 1712-1718.
13. T. Cai, Y. Chen, Y. Wang, H. Wang, X. Liu, Q. Jin, S. Agarwal and J. Ji, *Polym. Chem.*, 2014, **5**, 4061-4068.